



Air pollution in China: Status and spatiotemporal variations[☆]



Congbo Song^{a,1}, Lin Wu^{a,1}, Yaochen Xie^{b,1}, Jianjun He^c, Xi Chen^d, Ting Wang^a, Yingchao Lin^a, Taosheng Jin^a, Anxu Wang^a, Yan Liu^a, Qili Dai^a, Baoshuang Liu^a, Ya-nan Wang^a, Hongjun Mao^{a,*}

^a Center for Urban Transport Emission Research, State Environmental Protection Key Laboratory of Urban Ambient Air Particulate Matter Pollution Prevention and Control, College of Environmental Science and Engineering, Nankai University, Tianjin 300071, China

^b School of the Gifted Young, University of Science and Technology of China, Hefei 230026, China

^c State Key Laboratory of Severe Weather & Key Laboratory of Atmospheric Chemistry of CMA, Chinese Academy of Meteorological Sciences, Beijing 100081, China

^d Department of Occupational and Environmental Health, School of Public Health, Tianjin Medical University, Tianjin 300070, China

ARTICLE INFO

Article history:

Received 17 November 2016

Received in revised form

14 April 2017

Accepted 15 April 2017

Available online 5 May 2017

Keywords:

Air pollution

China

Spatial variation

Temporal variation

Major pollutant

ABSTRACT

In recent years, China has experienced severe and persistent air pollution associated with rapid urbanization and climate change. Three years' time series (January 2014 to December 2016) concentrations data of air pollutants including particulate matter (PM_{2.5} and PM₁₀) and gaseous pollutants (SO₂, NO₂, CO, and O₃) from over 1300 national air quality monitoring sites were studied to understand the severity of China's air pollution. In 2014 (2015, 2016), annual population-weighted-average (PWA) values in China were 65.8 (55.0, 50.7) μg m⁻³ for PM_{2.5}, 107.8 (91.1, 85.7) μg m⁻³ for PM₁₀, 54.8 (56.2, 57.2) μg m⁻³ for O_{3-8 h}, 39.6 (33.3, 33.4) μg m⁻³ for NO₂, 34.1 (26, 21.9) μg m⁻³ for SO₂, 1.2 (1.1, 1.1) mg m⁻³ for CO, and 0.60 (0.59, 0.58) for PM_{2.5}/PM₁₀, respectively. In 2014 (2015, 2016), 7% (14%, 19%), 17% (27%, 34%), 51% (67%, 70%) and 88% (97%, 98%) of the population in China lived in areas that meet the level of annual PM_{2.5}, PM₁₀, NO₂, and SO₂ standard metrics from Chinese Ambient Air Quality Standards-Grade II. The annual PWA concentrations of PM_{2.5}, PM₁₀, O_{3-8 h}, NO₂, SO₂, CO in the Northern China are about 40.4%, 58.9%, 5.9%, 24.6%, 96.7%, and 38.1% higher than those in Southern China, respectively. Though the air quality has been improving recent years, PM_{2.5} pollution in wintertime is worsening, especially in the Northern China. The complex air pollution caused by PM and O₃ (the third frequent major pollutant) is an emerging problem that threatens the public health, especially in Chinese mega-city clusters. NO_x controls were more beneficial than SO₂ controls for improvement of annual PM air quality in the northern China, central, and southwest regions. Future epidemiologic studies are urgently required to estimate the health impacts associated with multi-pollutants exposure, and revise more scientific air quality index standards.

© 2017 Elsevier Ltd. All rights reserved.

1. Introduction

Exposure to ambient air pollution has been associated with increased risks of mortality and morbidity worldwide (Cao et al., 2011; Chen et al., 2016; Dockery et al., 1993; Guan et al., 2016; Kampa and Castanas, 2008; Lepeule et al., 2012; Song et al., 2017; West et al., 2016; Zhang et al., 2014a; Zhou et al., 2014).

[☆] This paper has been recommended for acceptance by David Carpenter.

* Corresponding author.

E-mail address: hongjun_mao@126.com (H. Mao).

¹ Co-first authors.

According the Global Burden of Diseases (GBD) project, air pollution was responsible for 1.6 million deaths in China and 4.2 million deaths worldwide in 2015 (Forouzanfar et al., 2016; Landrigan, 2016). Severe and persistent air pollution in China is an immense burden for health care and economy (Chen et al., 2013; Guan et al., 2016; Guo et al., 2014; Huang et al., 2014a; Li et al., 2016c; Sun et al., 2014; Wang et al., 2016; Zhang et al., 2015). A recent study suggested that ambient fine particulate matter (PM_{2.5}) accounted for 15.5% (1.7 million) of all cause deaths in China in 2015 (Song et al., 2017). The costs of air pollution is so high that it can distort the health care spending and threaten sustainable development, and spread across large populations over many years and destroy natural resources (Landrigan, 2016; Xie et al., 2016).

In order to prevent further deterioration caused by air pollution, protect public health, and mitigate the effects of climate change, China has taken significant measures in recent years. Desulfurization of coal-fired power plants and the installation of selective catalytic reduction (SCR) systems were implemented in 2005 and 2011, respectively. At the same time, the strategies of upgrading fuels for vehicles and banning older polluting cars were introduced at the city-level (Wu et al., 2017). According to the 12th (2010–2015) China's Five-Year Plans (FYP), China targeted to cut 8% of sulfur dioxide (SO₂) and 10% of nitrogen dioxide (NO₂) emissions and reduce energy consumption by 16% and carbon dioxide (CO₂) intensity by 17% in 2015 from 2010 levels (Li et al., 2016c; Mao et al., 2014). Recent studies reported the effectiveness of government's regulations on SO₂ and nitrogen oxides (NO_x) emissions reductions in China (Liu et al., 2016b; van der A et al., 2017). The 'Air Pollution Prevention and Control Action Plan' was enacted by the Chinese government on September 10, 2013. It aimed to reduce heavily polluted days dramatically and significantly improve national air quality with long-term efforts. A new law on environmental protection, regarded as an important milestone in Chinese air pollution prevention, was implemented on January 1, 2015. According to the bulletin of the Chinese environment, the annual emissions of SO₂ and NO_x decreased 5.8% and 10.9%, respectively, in 2015 (He et al., 2017). Improvements in air quality in China during 2014–2015 were mostly attributed to these effective emission controls, although the meteorological conditions in 2015 were more unfavorable for pollutant dispersion than that in 2014 (He et al., 2017).

Within the 12th FYP, the New Chinese "Ambient air quality standard" (CAAQS) was published by the Ministry of Environmental Protection (MEP) and the General Administration of Quality Supervision, Inspection, and Quarantine of China in 2012 (He et al., 2017; Li et al., 2016b). For the first time, PM_{2.5} and 8-h ozone (O₃₋₈ h) were added into CAAQS. Additionally, China released the "Technical Regulation of Ambient Air Quality Index (HJ 633–2012)" (MEP, 2012) in 2012 to replace the air pollution index (API) with the air quality index (AQI). AQI is used to communicate to the public how serious the air pollution currently is and to help guide sensitive populations (children, the elderly, and people with heart or respiratory illness) through planning their outdoor activities. The MEP of China has started to grant access to air quality data (including PM_{2.5}, PM₁₀ (particulate matter with an aerodynamic diameter of less than 10 μm), O₃, NO₂, SO₂, and CO (carbon monoxide)) collected at the national air quality monitoring sites (NAQMS) of some major cities (<http://113.108.142.147:20035/emcpublish/>) since January 2013. Establishing a nation-wide real-time NAQMS network was proposed in the China's 13th FYP. The ground-based NAQMS network of mainland China contained 944 sites in 190 cities in 2014, 1494 sites in 367 cities in 2015, and 1467 sites in 367 cities in 2016. The intensive NAQMS network and relatively long time series (January 2014 to December 2016) analyzed in this study provided valuable insights into the status of the China's air pollution problem.

This study aims to analyze the air quality monitoring data from January 2014 to December 2016, and present the current status of air pollution in China. Population exposure, spatial and temporal variations of the air pollutants (PM_{2.5}, PM₁₀, O₃, NO₂, SO₂, CO), the major pollutants, the temporal evolution of polluted days, and correlations between air pollutants were investigated. The air pollution data collected at each NAQMS and the population data used in this study are available to the public for research purposes. The data, analysis procedures, and plotting scripts (ipython notebook) from this study are also available upon request the corresponding authors.

2. Materials and methods

2.1. Study areas

This study analyzed the air pollution data collected in 31 provinces of China, including the northern and southern China, four megacity clusters (BTH: Beijing-Tianjin-Hebei, YRD: Yangtze River Delta, PRD: Pearl River Delta, and CY: Cheng-Yu) (Fig. S1), and seven geographic regions (northeast, north, northwest, south, east, central and southwest) (Fig. 1), to better understand the spatial variations in concentrations across China. In this study, northern and southern China are divided based on the demarcation line of the Qinling Mountain and the eastern extension to the Huaihe River in central and eastern China (Chen et al., 2013; Zhou et al., 2016). Northern China includes the northeast (Heilongjiang, Jilin, Liaoning), north (Beijing, Tianjin, Hebei), Shanxi), and northwest (Shanxi, Gansu, Qinghai, Ningxia, Xinjiang, Inner Mongolia) provinces. Southern China includes the east (YRD (Shanghai, Jiangsu, Zhejiang), Anhui, Fujian, Jiangxi, Shandong), central (Henan, Hubei, Hunan), south (Guandong (PRD), Guangxi, Hainan), and southwest (CY (Sichuan, Chongqing), Guizhou, Tibet, and Yunnan) provinces.

2.2. Air quality data and quality control

To investigate the current status and spatiotemporal characteristics of ambient air pollution in China, air quality monitoring data (PM_{2.5}, PM₁₀, SO₂, NO₂, CO and O₃ concentrations) was collected at over 1300 NAQMS were analyzed from January 2014 to December 2016. Additional data (December 17 to 31, 2013, January 1 to 15, 2017) were included to calculate monthly moving average concentrations. The extra months (January to February 2017) were also included to calculate the air pollution status in wintertime of 2016. Quality assurance and quality control of the ground monitoring data have been reported in previous studies (Wang et al., 2014b; Zhao et al., 2016).

All downloaded data were pre-processed to reject spatial and temporal outliers. This was carried out by comparing every single values with the values from adjacent monitoring stations and with the time series data. Our removal criteria consisted of four conditions, three of which were consistent with previous studies (Barrero et al., 2015; He et al., 2017; Song et al., 2017). The time series of hourly concentrations were standardized using the z scores method. The points in the transformed time series meeting the following conditions were removed from the hourly raw data: (1) have an absolute z score of larger than 4 ($|z_t| > 4$), (2) have an increment from the previous value as larger than 9 ($z_t - z_{t-1} > 9$) with the previous value, (3) have a ratio of the value to its centered rolling mean of order 3 (RM3) larger than 2 ($z_t / \text{RM3}(z_t) > 2$), and (4) have an increment twice the value of the city-wide average of the increment for all monitoring stations (city ($z_t - z_{t-1}$)) (i.e., $(z_t - z_{t-1}) / \text{city}(z_t - z_{t-1}) > 2$). The numbers of the removed data points, changes of the mean values, and the percentage of valid data points at each NAQMS after pre-processing methods are provided in Tables S1 and Table S2. The overall monitoring efficiency are $91.8 \pm 14.2\%$ for PM_{2.5}, $85.0 \pm 15.1\%$ for PM₁₀, $91.4 \pm 14.4\%$ for O₃₋₁ h, $94.4 \pm 13.2\%$ for O₃₋₈ h, $91.9 \pm 14.3\%$ for NO₂, $92.1 \pm 14.1\%$ for SO₂, and $91.8 \pm 14.2\%$ for CO.

Annual average concentrations of the six criteria pollutants at each NAQMS were then computed from the hourly time series data when more than 80% of the measurements in a year were valid data (Table S2). The daily or hourly mass concentrations (PWAC) of air pollutants in the 31 provinces and other regions were represented by the daily population-weighted-average (PWA) concentrations in all cities within each province or region:

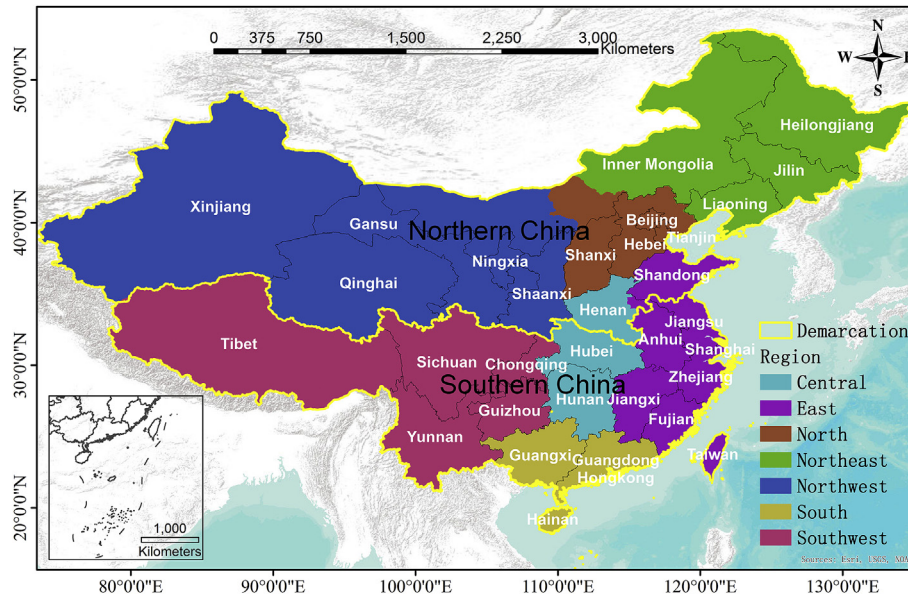


Fig. 1. Map of China. (The northern and southern China are divided by the yellow color solid line).

$$PWAC = \frac{\sum_{i=1}^n (C_i \times Pop_i)}{\sum_{i=1}^n Pop_i} \quad (1)$$

where C is the mass concentration of the air pollutants. Pop is the population number. The suffixes i represent different cities. n is the number of all cities within each province or region.

Daily Individual Air Quality Index (IAQI) of PWA concentrations of pollutants ($PM_{2.5}$, PM_{10} , SO_2 , NO_2 , CO , O_3_{1h} , and O_3_{8h}) in 31 provinces and regions were calculated based on the standards of air quality classification in “Technical Regulation of Ambient Air Quality Index (HJ 633-2012)”. A daily “major pollutant” was identified for every province or region to determine which pollutant contributes the most to the air quality degradation (the maximum IAQI among six pollutants with $IAQI > 50$, corresponding concentration limits of $PM_{2.5} > 35 \mu g m^{-3}$, $PM_{10} > 50 \mu g m^{-3}$, $O_3_{8h} > 100 \mu g m^{-3}$, $O_3_{1h} > 160 \mu g m^{-3}$, $NO_2 > 40 \mu g m^{-3}$, $SO_2 > 50 \mu g m^{-3}$, and $CO > 2 mg m^{-3}$). The pollutants with $IAQI > 100$ were defined as “non-attainment pollutants” with the corresponding concentration limits of $PM_{2.5} > 75 \mu g m^{-3}$, $PM_{10} > 150 \mu g m^{-3}$, $O_3_{8h} > 160 \mu g m^{-3}$, $O_3_{1h} > 200 \mu g m^{-3}$, $NO_2 > 80 \mu g m^{-3}$, $SO_2 > 150 \mu g m^{-3}$, and $CO > 4 mg m^{-3}$.

In this study, the default units of mass concentrations are $\mu g m^{-3}$ for $PM_{2.5}$, PM_{10} , SO_2 , NO_2 , O_3 , and $mg m^{-3}$ for CO . The ratios between pollutants ($PM_{2.5}/PM_{10}$ ratio, $PM_{2.5}/CO$ ratio, $PM_{2.5}/SO_2$ ratio, and SO_2/NO_2 ratio) are dimensionless values.

2.3. Population data

The population data in this study was obtained from the National Bureau of Statistics of the People's Republic of China. The latest census data were from the Sixth National Population Census which was carried out in 2010. Although some provincial capitals might have released their latest version of population data, we still used the 2010 population data for data integrity and consistency, considering that not all cities have the updated population data. The census data were at the county-level and summed up to the city-level for this study (Song et al., 2017).

2.4. Spatial analysis

The Pearson correlation coefficient (r) was used as an indicator of spatial pattern correlation between pairs of air pollutants. The spatial heterogeneity of observed concentrations in each region was investigated using coefficient of divergence (COD) (Sawvel et al., 2015; Wongphatarakul et al., 1998) as well as coefficient of variation (CV) (He et al., 2017). The COD method was generally used to present the similarities between two datasets, and defined as follows:

$$COD_{jk} = \sqrt{\frac{1}{p} \sum_{i=1}^p \left(\frac{x_{ij} - x_{ik}}{x_{ij} + x_{ik}} \right)^2}$$

where x_{ij} represents the mass concentration for time i at NAQMS j , j and k represent two datasets, and p is the number of observations. If the two datasets are similar, the COD approaches zero. If the two datasets are very different, the COD approaches one. Before COD analysis, the set of diurnal variations at all sites within the region was split into two clusters (i.e., high and low cluster) by K-means clustering method (Zhao et al., 2016). The K-means clustering split the existing multidimensional data into predefined number of subgroups (clusters), which are as different as possible from each other, but as homogeneous as possible within themselves, by iteratively minimizing the sum of squared Euclidean distances from each member to its cluster centroids. Spatial variations were then quantified by COD between the two representative cluster centroids.

The method of coefficient of variation (CV, i.e., standard deviation divided (STD) by the mean value (\bar{x})) was also used to describe the degree of the spatial variations of air pollutant concentrations in Chinese regions, expressed by:

$$CV = \frac{STD}{\bar{x}} \quad (2)$$

2.5. Temporal analysis

Monthly moving average method was used to present the temporal variations of air pollutants. Diurnal variations of PWA concentrations of the six criteria pollutants in China were also analyzed. To better investigate the concentration-variations and formation (or emission)-process of the six criteria pollutants, diurnal variations of change-rates of PWA concentrations of the six criteria pollutants were also conducted, expressed by (Liu et al., 2016a; Zou et al., 2015):

$$\frac{d[X]}{dt} = [X]_{t+1} - [X]_t \quad (3)$$

where $[X]_t$ represents the PWA concentrations of air pollutants at time t , and $[X]_{t+1}$ represents the PWA concentrations for the next hour following time t .

The daily IAQI was calculated based on the “Technical Regulation of Ambient Air Quality Index (HJ 633–2012)” published by the Ministry of Environmental Protection. The counting statistic was used to investigate the days of major air pollutants, and the temporal evolution of non-attainment days of each air pollutant.

3. Results and discussion

3.1. Overview of air pollutants

This study analyzed the annual average mass concentrations of the pollutants at each NAQMS during 2014–2016 (Table S3). Table 1 and Table S4 summarize the annual averages and standard deviations of PWA concentrations of the six air pollutants and their ratios in 31 provinces during 2014–2016, respectively. In 2014 (2015, 2016), annual PWA values were 65.8 (55.0, 50.7) $\mu\text{g m}^{-3}$ for $\text{PM}_{2.5}$, 107.8 (91.1, 85.7) $\mu\text{g m}^{-3}$ for PM_{10} , 54.8 (56.2, 57.2) $\mu\text{g m}^{-3}$ for O_3 8 h, 39.6 (33.3, 33.4) $\mu\text{g m}^{-3}$ for NO_2 , 34.1 (26, 21.9) $\mu\text{g m}^{-3}$ for SO_2 , 1.2 (1.1, 1.1) mg m^{-3} for CO, 0.60 (0.59, 0.58) for $\text{PM}_{2.5}/\text{PM}_{10}$, and 0.83 (0.76, 0.65) for SO_2/NO_2 , respectively. According to the China Ministry of Environmental Protection, the annual average concentrations in 113 major cities in 2009 were 87 $\mu\text{g m}^{-3}$ for PM_{10} , 42 $\mu\text{g m}^{-3}$ for SO_2 , and 38 $\mu\text{g m}^{-3}$ for NO_2 (Kan et al., 2012). The annual PWA concentration of SO_2 declined significantly from 42 $\mu\text{g m}^{-3}$ (2009) to 21.9 $\mu\text{g m}^{-3}$ (2016) owing to the nationwide implementation of desulfurization systems (van der A et al., 2017). As a result of the regulations of NO_x emissions from power plants and heavy industry, the annual PWA concentration of NO_2 exhibited a decreasing trend only in recent years, consistent with satellite observations and emission inventories (Liu et al., 2016b; van der A et al., 2017). Our results suggested that approximately 59% (58–60%) in mass of PM_{10} in China is composed of $\text{PM}_{2.5}$, which is close to the ratios of 65% determined based on a literature review in China before 2012 (Zhou et al., 2016) and in London during 2006–2007 (Harrison et al., 2012; Zhang et al., 2015), 58% in 31 Chinese provincial capital cities during 2014–2015 (He et al., 2017), and 56% in 190 cities in China during 2013–2014 (Zhang and Cao, 2015).

Significant spatial differences in air pollutants concentrations among cities were observed. In 2014 (2015, 2016), the ranges of annual average values were 19.0–130.6 (10.7–119.1, 10.6–157.2) $\mu\text{g m}^{-3}$ for $\text{PM}_{2.5}$, 35.5–235.5 (25.7–335.7, 23.9–435.7) $\mu\text{g m}^{-3}$ for PM_{10} , 28.1–92.0 (28.7–96.8, 29.6–95.0) $\mu\text{g m}^{-3}$ for O_3 8 h, 12.9–66.4 (7.9–61.6, 8.7–61.0) $\mu\text{g m}^{-3}$ for NO_2 , 2.4–118.1 (3.3–82.6, 3.0–83.2) $\mu\text{g m}^{-3}$ for SO_2 , and 0.47–2.42 (0.23–2.72, 0.38–2.53) mg m^{-3} for CO. The cumulative population distribution of the annual values of $\text{PM}_{2.5}$, PM_{10} , O_3 , NO_2 , SO_2 , CO, $\text{PM}_{2.5}/\text{PM}_{10}$, $\text{PM}_{2.5}/\text{CO}$, $\text{PM}_{2.5}/\text{SO}_2$, and SO_2/NO_2 during the study period was

investigated to better understand the population exposure to air pollution in China (Fig. 2). In 2014 (2015, 2016), half population of China were exposed to annual average values higher than 63.6 (54.3, 47.2) $\mu\text{g m}^{-3}$ for $\text{PM}_{2.5}$, 103.8 (85.8, 77.2) $\mu\text{g m}^{-3}$ for PM_{10} , 54.3 (56.1, 56.9) $\mu\text{g m}^{-3}$ for O_3 8 h, 39.7 (33.3, 33.1) $\mu\text{g m}^{-3}$ for NO_2 , 27.8 (22.3, 18.4) $\mu\text{g m}^{-3}$ for SO_2 , and 1.11 (1.04, 0.96) mg m^{-3} for CO, respectively. In 2014 (2015, 2016), 7% (14%, 19%), 17% (27%, 34%), 51% (67%, 70%), and 88% (97%, 98%) of the population lived in areas met that meet the annual $\text{PM}_{2.5}$, PM_{10} , NO_2 , and SO_2 standards of CAAQS Grade II. The entire population of China were exposed to $\text{PM}_{2.5}$ concentrations above World Health Organization (WHO) air quality guidelines (AQG) of 10 $\mu\text{g m}^{-3}$.

3.2. Spatial variations

Fig. 3 shows the spatial distributions of annual average mass concentrations of the six air pollutants ($\text{PM}_{2.5}$, PM_{10} , O_3 8 h, NO_2 , SO_2 , and CO) at each NAQMS across China. Elevated concentrations were recorded at monitoring sites located in the northern China because of the high emissions from fossil fuel combustion and biomass burning (Hu et al., 2014; Wang et al., 2014b; Zhang and Cao, 2015; Zhao et al., 2016). Generally, air pollution in northern China is more severe than in southern China (He et al., 2017) due to distinct emissions sources, topographic features, and climate. Chen et al. (2013) reported that ambient concentrations of total suspended particulates (TSPs) were 184 $\mu\text{g m}^{-3}$ or 55% higher in northern China than in southern China during 1981–2000. During our study period (2014–2016), the annual PWA concentrations of $\text{PM}_{2.5}$, PM_{10} , O_3 8 h, NO_2 , SO_2 , and CO in northern China were 40.4 (39.9–41.0)%, 58.9 (57.0–59.9)%, 5.9 (2.6–8.3)%, 24.6 (24.0–25.2)%, 96.7 (86.3–115.1)%, and 38.1 (30.0–44.4)% higher than in southern China, respectively. The range in parentheses represents the minimum and maximum values during 2014–2016. The health impacts of the sustained exposure to multi-pollutants from China's Huai River policy could be reevaluated using these results and health data from China's Disease Surveillance Points (DSPs) system (Chen et al., 2013). The annual PWA concentrations of pollutants meeting the CAAQS Grade II standards are highlighted in bold in Table 1. For $\text{PM}_{2.5}$, only four provinces (Fujian: 33.2 $\mu\text{g m}^{-3}$, Hainan: 21.8 $\mu\text{g m}^{-3}$, Tibet: 23.8 $\mu\text{g m}^{-3}$, and Yunnan: 33.4 $\mu\text{g m}^{-3}$) in 2014, six provinces (Fujian: 28.8 $\mu\text{g m}^{-3}$, Guangdong: 34 $\mu\text{g m}^{-3}$, Hainan: 20.3 $\mu\text{g m}^{-3}$, Guizhou: 32.9 $\mu\text{g m}^{-3}$, Tibet: 26.7 $\mu\text{g m}^{-3}$, and Yunnan: 29.7 $\mu\text{g m}^{-3}$) and PRD (34.9 $\mu\text{g m}^{-3}$) in 2015, and six provinces (Fujian: 27.4 $\mu\text{g m}^{-3}$, Guangdong: 32 $\mu\text{g m}^{-3}$, Hainan: 18.8 $\mu\text{g m}^{-3}$, Guizhou: 33.5 $\mu\text{g m}^{-3}$, Tibet: 27.9 $\mu\text{g m}^{-3}$, and Yunnan: 28.2 $\mu\text{g m}^{-3}$) and two regions (South China: 33.4 $\mu\text{g m}^{-3}$, PRD: 32.8 $\mu\text{g m}^{-3}$) in 2016, meet the CAAQS Grade II of 35 $\mu\text{g m}^{-3}$. PRD is the first megacity cluster in meeting the limit value of 35 $\mu\text{g m}^{-3}$ of $\text{PM}_{2.5}$ in 2015. Spatial pattern of annual average mass concentration of PM_{10} (Fig. 2b) were similar to those of $\text{PM}_{2.5}$ (Fig. 2a) consistent with the strong correlation (Fig. S2, $r = 0.89$, $p < 0.05$) between their annual average mass concentrations.

Surface O_3 is a complex secondary pollutant produced in the atmosphere by complex, nonlinear, and temperature-dependent chemical reactions (Pusede et al., 2015). No clear spatial patterns were observed for annual concentration of both O_3 8 h (Fig. 3c) and O_3 1 h (Fig. S3) across China, which agrees with the findings of Chai et al. (2014) and Wang et al. (2014b). Previous studies found strong inverse relationships between O_3 and NO_x (Clapp and Jenkin, 2001; Song et al., 2016). However, in this study, negative correlations ($r = -0.19$, $p < 0.05$) were detected between the annual average concentrations of O_3 and NO_2 at each NAQMS across China (Fig. S4), suggesting that VOCs reactivity under a wide range of temperatures in China made ozone production difficult to effectively control (Fu et al., 2015; Pusede et al., 2014).

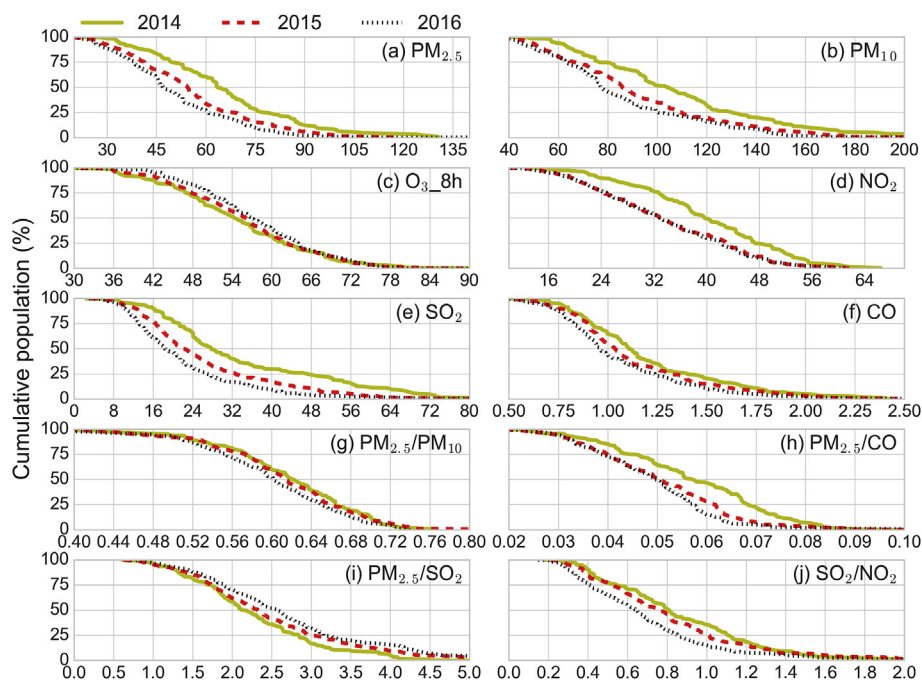


Fig. 2. Cumulative distribution of annual average mean of air pollutants and ratios in China.

Fig. 3d shows that high NO_2 and CO concentrations are mostly distributed over north and east China, which agrees with recent satellite observations (van der A et al., 2017). Traffic emissions are an important source of NO_x and CO in Chinese cities, contributing 53% and 20% to total NO_x and CO emissions in Beijing (He et al., 2016b, 2017; Jing et al., 2016), respectively, and 25% to total NO_2 emissions in China in 2010 according to the MEIC (Multi-resolution emission inventory for China) inventory (Liu et al., 2016b; van der A et al., 2017). NO_2 and CO are also the precursors of O_3 in the complex atmospheric chemistry. NO_x controls are most beneficial at locations with a high exceedance probability of O_3 standards (Pusede et al., 2015). Recent studies suggested that NO_2 column densities of China peaked in 2011 and decreased by 32% from 2011 to 2015 because of the reductions in emissions from power plants with the implementation of selective catalytic reduction (SCR) systems (Liu et al., 2016b; van der A et al., 2017).

For SO_2 , Shanxi and Ningxia provinces were the two hotspots (Fig. 3e) with concentrations (Shanxi: $65.2 \mu\text{g m}^{-3}$ in 2016, Ningxia: $63.7 \mu\text{g m}^{-3}$ in 2014) exceeding the limit value of $60 \mu\text{g m}^{-3}$. A recent study suggested that newly built power plants in 2012 causes a strong increase in both SO_2 and NO_x in Ningxia province (van der A et al., 2017). The annual PWA concentrations of SO_2 in Shanxi province ($56.5 \mu\text{g m}^{-3}$ in 2014, $59.6 \mu\text{g m}^{-3}$ in 2015, and $65.2 \mu\text{g m}^{-3}$ in 2016) were 65.7% in 2014, 129.2% in 2015, and 197.7% in 2016, higher than the overall national average in 2014, 2015, and 2016, respectively. The SO_2 oxidation process was considered as a key factor in the formation of persistent severe haze in China (Wang et al., 2016). Additionally, SO_2 was found to have significant effects on mortality after adjustment for TSP in a Chinese cohort study (Cao et al., 2011) and was associated with increased risk of lung cancer mortality in single-pollution models in Northern China (Chen et al., 2016). Long-term and short-term health endpoints associated with high concentrations of SO_2 in Shanxi and Ningxia provinces should be further investigated in future studies.

Fig. 4 shows the spatial distributions of annual average ratios between the air pollutants ($\text{PM}_{2.5}/\text{PM}_{10}$, $\text{PM}_{2.5}/\text{CO}$, $\text{PM}_{2.5}/\text{SO}_2$, and

SO_2/NO_2) at each NAQMS across China. The annual PWA values of $\text{PM}_{2.5}/\text{PM}_{10}$ in northern China were 13.1 (12.5–14.3) % lower than Southern China. Coarse particulate matters were more abundant in the northern China that have less vegetation cover and lower humidity than southern China (Song et al., 2017; Xu et al., 2015). The ratios of $\text{PM}_{2.5}$ to CO (CO is an indicator of primary combustion sources) was calculated to investigate the spatial variations of secondary formation of $\text{PM}_{2.5}$ across China (Fig. 4b) (He et al., 2017; Zhang and Cao, 2015). During the study period, the PWA $\text{PM}_{2.5}/\text{CO}$ were the highest in the north (0.075), followed by the east (0.072), central (0.069), southwest (0.068), northeast (0.065), northwest (0.057), and south (0.049). Based on source apportionment results, the concentration of secondary aerosol is large in the northeast, north, central, and east (He et al., 2017; Song et al., 2017). As for the mega-city clusters, the ratios were the highest in the BTH (0.035), followed by CY (0.032), YRD (0.026) and PRD (0.018). These results suggest high secondary contribution to $\text{PM}_{2.5}$ were found in the north and east China, and in BTH and CY mega-city clusters (Guo et al., 2014; Hu et al., 2017; Huang et al., 2014a; Sun et al., 2014; Wang et al., 2016). SO_2 can be used to normalize $\text{PM}_{2.5}$ to exclude the effects of coal combustion and meteorological conditions. Fig. 4c illustrates the spatial patterns of $\text{PM}_{2.5}/\text{SO}_2$ across China. Among Chinese provinces, highest $\text{PM}_{2.5}/\text{SO}_2$ was 7.3 (4.0–12.4) in Beijing, followed by 5.3 (3.8–7.7) in Hainan, 5.2 (2.7–9.2) in Xinjiang, 4.9 (2.5–9.4) in Hubei, 4.5 (2.7–7.5) in Chongqing, and 4.3 (3.0–6.7) in Sichuan provinces. The $\text{PM}_{2.5}/\text{SO}_2$ in Beijing was 150% (109%–177%) higher than the overall national average, showing the strong contribution of traffic-related emissions to $\text{PM}_{2.5}$ in Beijing consistent with previous studies (He et al., 2016b; Jing et al., 2016; Ziková et al., 2016). The SO_2/NO_2 ratio is an indicator of air pollution from stationary and mobile sources (Aneja et al., 2001; Nirel and Dayan, 2001). The Shanxi and Ningxia provinces showed highest SO_2/NO_2 ratios in China, suggesting that air pollution in those two provinces was originated from local industrial sources and coal combustion (van der A et al., 2017). Lowest SO_2/NO_2 was observed in Beijing (0.26, 0.2–0.34),

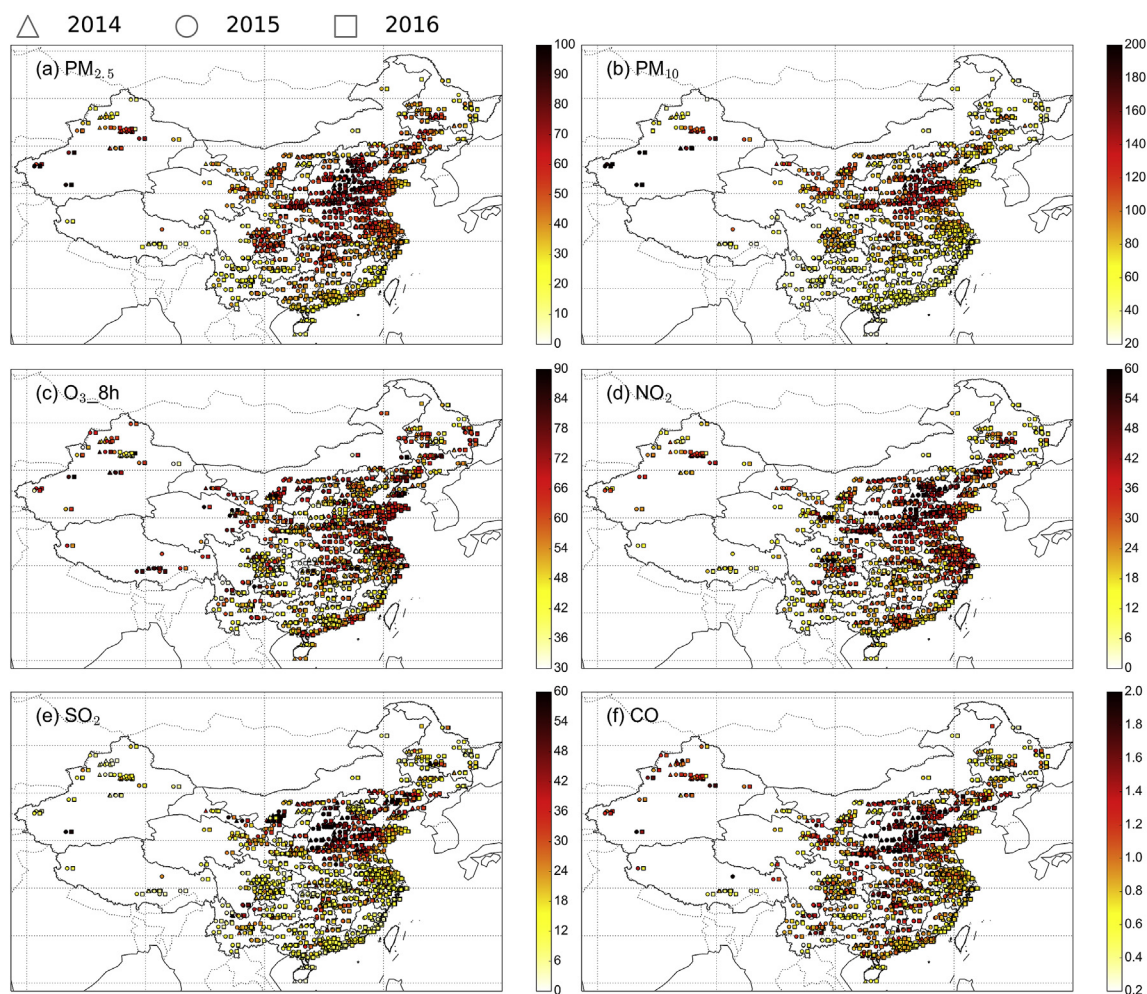


Fig. 3. Spatial distribution of site-specific annual mass concentrations of each air pollutant (the longitude of NAQMS in 2014 and 2016 were shifted to left side (-0.7°) and right side ($+0.7^\circ$) of those in 2015, respectively). The units of mass concentrations are $\mu\text{g m}^{-3}$ for $\text{PM}_{2.5}$, PM_{10} , SO_2 , NO_2 , O_3 _8 h, and mg m^{-3} for CO.

followed by Hainan (0.38, 0.35–0.40), Shanghai (0.39, 0.37–0.41), and Fujian (0.41, 0.37–0.44). These results confirm that air pollution in Beijing, Hainan, Shanghai, and Fujian is strongly associated with vehicle emissions.

A previous study suggested that spatial variations in 31 major Chinese cities were the largest for SO_2 (CV = 60%), followed by $\text{PM}_{2.5}$ (CV = 33%), PM_{10} (CV = 32%), CO (CV = 26%), NO_2 (CV = 25%), and O_3 (CV = 19%) (He et al., 2017). However, these results do not represent the overall spatial variations of air pollutant concentrations because 31 major Chinese cities are only less than one-tenth of all Chinese cities. In this study, based on the annual average mass concentrations of air pollutants at over 1300 NAQMS during the three-year period, spatial variations (Table S5) were the largest for SO_2 (CV = 65.1%), followed by PM_{10} (CV = 40.1%), NO_2 (CV = 38.3%), $\text{PM}_{2.5}$ (CV = 36.7%), CO (CV = 35.5%), and O_3 _8 h (CV = 23.4%). The largest spatial variation was observed in the southwest for $\text{PM}_{2.5}$ (CV = 39.0%) and NO_2 (CV = 43.3%), northwest for PM_{10} (CV = 40.8%), O_3 _8 h (CV = 27.5%), and SO_2 (CV = 65.5%), and northeast of China for CO (CV = 37.0%). Additionally, the largest coefficient of divergence (Table S6) was observed in the southwest for $\text{PM}_{2.5}$ (COD = 0.34) and NO_2 (COD = 0.34), northwest for PM_{10} (COD = 0.45), O_3 _8 h (COD = 0.24), and SO_2 (COD = 0.51), and northeast of China for CO (COD = 0.32). The results of spatial variations from CV method is in agreement with those from COD method.

3.3. Temporal variations

The three-year time series of PWA values of mass concentrations and ratios in Chinese mega-city clusters and seven geographic regions showed significant seasonal variations (Fig. 5 and S5). Changes in monthly moving average concentrations of PM ($\text{PM}_{2.5}$ and PM_{10}), NO_2 , SO_2 , and CO conform to U-shaped patterns with the highest in the winter (December to February) and the lowest in the summer (June to August) (Wang et al., 2014b, 2017a). The elevated PWA concentrations in wintertime were a result of the combination of coal combustion and biomass burning for residential heating, and the stagnant meteorological conditions that limit the dilution and dispersion of air pollutants (Chai et al., 2014; Jeong and Park, 2017; Liu et al., 2017; Sun et al., 2014; Wang et al., 2014a; Yang et al., 2016). Although annual PWA $\text{PM}_{2.5}$ concentrations in China were decreasing during this study period (see Fig. 2), PWA $\text{PM}_{2.5}$ concentrations in the winter of 2016 in the Northern China (including BTH, North, Northwest) and China were observed to be higher than that in the winter of 2014 and 2015 (Tables S7 and S8), likely due to weaker monsoon and higher secondary aerosols in wintertime over East Asia recent years (Huang et al., 2014a; Jeong and Park, 2017).

Eight-hour O_3 concentrations in all regions exhibit mountain-peak-shaped patterns (opposite to U-shaped patterns) with the highest concentrations in the summer and the lowest in the winter,

Table 1
Annual average PWC of six air pollutants and ratios between pollutants in 31 provinces during 2014–2016.^a

| Regions | PM _{2.5} | | | PM ₁₀ | | | O ₃ -8 h | | | NO ₂ | | | SO ₂ | | | CO | | | PM _{2.5} /PM ₁₀ | | | SO ₂ /NO ₂ | | |
|------------------|-------------------|-------------|----------------|------------------|-------------|-------------|---------------------|------|------|-----------------|-------------|-------------|-----------------|-------------|-------------|------|------|------|-------------------------------------|------|------|----------------------------------|------|------|
| | 2014 | 2015 | 2016 | 2014 | 2015 | 2016 | 2014 | 2015 | 2016 | 2014 | 2015 | 2016 | 2014 | 2015 | 2016 | 2014 | 2015 | 2016 | 2014 | 2015 | 2016 | 2014 | 2015 | 2016 |
| China | 65.8 | 55.0 | 50.7 | 107.8 | 91.1 | 85.7 | 54.8 | 56.2 | 57.2 | 39.6 | 33.3 | 33.4 | 34.1 | 26.0 | 21.9 | 1.2 | 1.1 | 1.1 | 0.60 | 0.59 | 0.58 | 0.83 | 0.76 | 0.65 |
| Northern | 78.2 | 66.0 | 60.6 | 135.0 | 116.1 | 109.2 | 55.6 | 58.3 | 59.9 | 44.4 | 37.7 | 37.7 | 48.4 | 35.4 | 30.0 | 1.4 | 1.3 | 1.3 | 0.56 | 0.56 | 0.54 | 1.04 | 0.90 | 0.76 |
| Northeast | 59.1 | 51.5 | 41.7 | 99.1 | 85.2 | 70.9 | 53.1 | 56.8 | 58.4 | 38.6 | 32.1 | 29.0 | 43.4 | 32.2 | 25.9 | 1.1 | 1.0 | 1.0 | 0.57 | 0.58 | 0.58 | 1.05 | 0.90 | 0.83 |
| -Heilongjiang | 58.0 | 46.0 | 37.3 | 89.6 | 73.6 | 60.7 | 45.7 | 51.0 | 48.3 | 38.5 | 30.7 | 27.6 | 39.8 | 26.0 | 20.2 | 0.9 | 0.8 | 0.8 | 0.60 | 0.60 | 0.58 | 0.93 | 0.76 | 0.69 |
| -Jilin | 63.6 | 55.6 | 42.3 | 107.8 | 90.6 | 71.4 | 56.6 | 59.6 | 60.5 | 40.9 | 33.7 | 29.7 | 31.2 | 27.8 | 22.3 | 1.0 | 0.9 | 0.9 | 0.55 | 0.59 | 0.58 | 0.77 | 0.76 | 0.70 |
| -Liaoning | 60.2 | 55.9 | 46.6 | 101.3 | 92.7 | 79.9 | 57.8 | 60.1 | 64.9 | 40.0 | 34.8 | 32.1 | 48.5 | 41.7 | 34.9 | 1.3 | 1.2 | 1.1 | 0.58 | 0.59 | 0.58 | 1.16 | 1.09 | 1.02 |
| North | 87.0 | 75.6 | 68.1 | 148.9 | 129.0 | 118.0 | 60.2 | 61.3 | 61.0 | 47.6 | 43.2 | 43.5 | 52.2 | 38.6 | 30.8 | 1.4 | 1.4 | 1.3 | 0.57 | 0.57 | 0.56 | 1.06 | 0.86 | 0.70 |
| -BTH | 97.7 | 81.0 | 74.9 | 161.8 | 133.3 | 121.7 | 54.7 | 54.7 | 55.4 | 51.3 | 47.5 | 50.3 | 50.3 | 36.9 | 29.9 | 1.6 | 1.5 | 1.4 | 0.58 | 0.59 | 0.59 | 0.92 | 0.73 | 0.58 |
| -Beijing | 85.2 | 79.4 | 71.9 | 121.9 | 108.7 | 98.9 | 57.6 | 59.2 | 56.8 | 55.2 | 48.4 | 46.4 | 21.1 | 13.3 | 9.8 | 1.3 | 1.3 | 1.1 | 0.65 | 0.71 | 0.69 | 0.34 | 0.24 | 0.20 |
| -Tianjin | 86.9 | 71.3 | 70.4 | 136.2 | 120.5 | 108.3 | 50.4 | 47.7 | 50.3 | 55.0 | 42.1 | 49.6 | 48.3 | 29.2 | 21.4 | 1.7 | 1.4 | 1.4 | 0.62 | 0.58 | 0.63 | 0.82 | 0.62 | 0.42 |
| -Hebei | 103.7 | 83.4 | 76.5 | 179.1 | 145.0 | 131.4 | 54.5 | 54.8 | 56.0 | 50.0 | 48.3 | 51.4 | 58.6 | 44.8 | 36.8 | 1.7 | 1.6 | 1.5 | 0.56 | 0.56 | 0.56 | 1.10 | 0.88 | 0.69 |
| -Shanxi | 61.6 | 56.8 | 59.8 | 113.5 | 98.2 | 107.5 | 45.4 | 52.8 | 52.5 | 35.0 | 32.7 | 35.4 | 56.5 | 59.6 | 65.2 | 1.9 | 1.9 | 1.8 | 0.54 | 0.57 | 0.54 | 1.54 | 1.70 | 1.66 |
| Northwest | 64.7 | 53.6 | 57.5 | 126.9 | 109.6 | 117.9 | 42.6 | 54.7 | 56.6 | 38.8 | 32.4 | 34.7 | 39.9 | 33.9 | 32.9 | 1.6 | 1.4 | 1.4 | 0.50 | 0.49 | 0.49 | 0.97 | 0.99 | 0.88 |
| -Shanxi | 70.8 | 53.5 | 60.6 | 133.7 | 103.0 | 113.8 | 39.5 | 49.0 | 53.6 | 40.3 | 35.6 | 40.1 | 30.9 | 20.9 | 18.4 | 1.5 | 1.5 | 1.3 | 0.51 | 0.51 | 0.52 | 0.71 | 0.57 | 0.45 |
| -Gansu | 55.1 | 41.8 | 38.7 | 121.6 | 91.3 | 86.6 | 46.7 | 60.8 | 63.6 | 39.8 | 32.0 | 30.9 | 29.4 | 27.7 | 23.5 | 1.4 | 1.1 | 1.0 | 0.48 | 0.47 | 0.47 | 0.75 | 0.81 | 0.73 |
| -Qinghai | 61.4 | 46.3 | 41.9 | 118.1 | 91.8 | 95.5 | 40.5 | 67.3 | 59.7 | 33.6 | 27.7 | 29.8 | 36.8 | 24.2 | 22.2 | 1.3 | 1.1 | 1.2 | 0.56 | 0.54 | 0.47 | 1.09 | 0.87 | 0.75 |
| -Ningxia | 47.9 | 46.0 | 45.0 | 110.2 | 104.5 | 99.9 | 52.5 | 54.2 | 63.5 | 36.1 | 25.7 | 26.7 | 63.7 | 39.0 | 37.8 | 1.1 | 0.9 | 0.9 | 0.45 | 0.45 | 0.48 | 1.66 | 1.41 | 1.33 |
| -Xinjiang | 62.9 | 68.1 | 80.6 | 157.7 | 171.8 | 196.0 | 40.1 | 55.4 | 56.3 | 49.5 | 31.1 | 33.5 | 23.5 | 21.4 | 17.2 | 1.3 | 1.3 | 1.4 | 0.41 | 0.42 | 0.42 | 0.45 | 0.69 | 0.50 |
| -InnerMongolia | 44.6 | 41.8 | 36.0 | 113.9 | 86.6 | 76.1 | 53.0 | 60.9 | 64.2 | 34.9 | 27.1 | 26.1 | 47.1 | 28.8 | 22.7 | 1.2 | 0.9 | 0.9 | 0.39 | 0.48 | 0.48 | 1.29 | 0.99 | 0.85 |
| Southern | 55.9 | 46.8 | 43.2 | 86.0 | 72.6 | 68.3 | 54.2 | 54.6 | 55.3 | 35.8 | 30.1 | 30.3 | 22.5 | 19.0 | 15.9 | 1.0 | 1.0 | 0.9 | 0.64 | 0.64 | 0.63 | 0.63 | 0.63 | 0.54 |
| East | 58.0 | 49.6 | 45.5 | 90.1 | 76.6 | 72.0 | 59.1 | 57.9 | 59.2 | 38.5 | 33.7 | 34.0 | 23.4 | 20.8 | 17.8 | 0.9 | 0.9 | 0.9 | 0.64 | 0.64 | 0.62 | 0.61 | 0.63 | 0.55 |
| -YRD | 60.3 | 54.1 | 46.6 | 92.6 | 83.9 | 75.1 | 61.4 | 64.4 | 63.7 | 40.7 | 39.9 | 38.0 | 24.1 | 21.1 | 17.4 | 0.9 | 0.9 | 0.9 | 0.65 | 0.64 | 0.61 | 0.59 | 0.54 | 0.48 |
| -Shanghai | 53.0 | 53.9 | 45.5 | 74.8 | 74.0 | 62.7 | 68.5 | 72.5 | 72.1 | 44.2 | 45.6 | 42.9 | 18.0 | 17.0 | 14.4 | 0.8 | 0.9 | 0.8 | 0.71 | 0.72 | 0.71 | 0.41 | 0.39 | 0.37 |
| -Jiangsu | 66.0 | 57.7 | 50.1 | 104.4 | 94.7 | 84.6 | 61.2 | 65.3 | 64.6 | 39.2 | 38.1 | 37.7 | 28.5 | 24.9 | 21.0 | 1.0 | 1.0 | 1.0 | 0.63 | 0.60 | 0.58 | 0.73 | 0.66 | 0.59 |
| -Zhejiang | 54.4 | 47.6 | 41.4 | 81.4 | 71.0 | 65.9 | 58.5 | 58.8 | 57.8 | 41.9 | 39.3 | 36.2 | 21.3 | 16.7 | 13.3 | 0.9 | 0.9 | 0.8 | 0.67 | 0.67 | 0.62 | 0.50 | 0.43 | 0.39 |
| -Anhui | 76.3 | 56.7 | 55.0 | 108.9 | 82.6 | 80.7 | 38.0 | 50.1 | 57.9 | 28.0 | 30.7 | 36.7 | 21.9 | 22.0 | 20.0 | 1.1 | 1.0 | 0.9 | 0.71 | 0.68 | 0.67 | 0.80 | 0.74 | 0.56 |
| -Fujian | 33.2 | 28.8 | 27.4 | 63.2 | 50.1 | 48.0 | 55.8 | 50.7 | 49.1 | 27.9 | 24.0 | 24.0 | 9.9 | 10.3 | 9.3 | 0.7 | 0.8 | 0.7 | 0.52 | 0.57 | 0.57 | 0.37 | 0.44 | 0.41 |
| -Jiangxi | 47.6 | 42.5 | 44.0 | 81.0 | 64.6 | 69.4 | 45.6 | 49.4 | 53.5 | 30.0 | 23.5 | 23.9 | 28.5 | 27.0 | 23.1 | 0.9 | 1.0 | 1.0 | 0.59 | 0.66 | 0.64 | 0.95 | 1.19 | 1.02 |
| -Shandong | 79.7 | 74.2 | 64.9 | 138.7 | 129.7 | 118.3 | 66.0 | 67.6 | 66.1 | 44.6 | 40.4 | 38.1 | 54.8 | 41.3 | 32.2 | 1.3 | 1.3 | 1.2 | 0.57 | 0.56 | 0.54 | 1.20 | 1.01 | 0.84 |
| Central | 79.2 | 68.3 | 60.5 | 124.3 | 110.0 | 100.6 | 49.1 | 56.1 | 59.2 | 40.7 | 33.4 | 33.0 | 38.6 | 27.4 | 22.2 | 1.4 | 1.3 | 1.2 | 0.63 | 0.61 | 0.59 | 0.93 | 0.82 | 0.68 |
| -Henan | 83.3 | 80.4 | 72.1 | 135.7 | 135.6 | 126.3 | 52.2 | 58.2 | 63.6 | 44.7 | 39.3 | 39.6 | 48.1 | 34.6 | 29.4 | 1.6 | 1.4 | 1.4 | 0.60 | 0.59 | 0.56 | 1.04 | 0.87 | 0.74 |
| -Hubei | 86.4 | 66.4 | 55.1 | 129.6 | 100.1 | 87.0 | 53.2 | 56.5 | 57.3 | 45.6 | 32.7 | 31.4 | 35.2 | 19.1 | 13.8 | 1.3 | 1.2 | 1.1 | 0.67 | 0.65 | 0.62 | 0.76 | 0.57 | 0.44 |
| -Hunan | 68.7 | 52.9 | 48.2 | 104.9 | 82.1 | 75.3 | 41.3 | 52.9 | 54.7 | 31.8 | 25.7 | 24.8 | 28.3 | 24.1 | 19.0 | 1.2 | 1.1 | 1.0 | 0.65 | 0.63 | 0.63 | 0.90 | 0.97 | 0.79 |
| South | 42.7 | 35.9 | 33.4 | 63.9 | 54.9 | 51.3 | 56.5 | 53.3 | 51.9 | 30.4 | 26.0 | 26.4 | 17.7 | 14.7 | 12.7 | 1.0 | 1.0 | 0.9 | 0.65 | 0.64 | 0.64 | 0.60 | 0.58 | 0.51 |
| -Guangdong | 41.3 | 34.0 | 32.0 | 61.5 | 52.3 | 49.2 | 56.5 | 53.7 | 52.2 | 30.9 | 28.3 | 28.8 | 17.4 | 13.2 | 11.4 | 1.1 | 0.9 | 0.9 | 0.66 | 0.64 | 0.64 | 0.59 | 0.49 | 0.42 |
| -PRD | 42.7 | 34.9 | 32.8 | 63.8 | 54.1 | 50.7 | 54.5 | 49.9 | 50.1 | 38.8 | 35.2 | 35.9 | 17.7 | 13.2 | 11.2 | 1.0 | 0.9 | 0.9 | 0.65 | 0.63 | 0.64 | 0.47 | 0.39 | 0.33 |
| -Guangxi | 55.3 | 41.2 | 37.4 | 83.0 | 62.1 | 56.8 | 58.1 | 52.3 | 51.0 | 30.0 | 21.6 | 21.6 | 21.6 | 18.5 | 15.9 | 1.1 | 1.1 | 0.9 | 0.65 | 0.65 | 0.65 | 0.73 | 0.88 | 0.77 |
| -Hainan | 21.8 | 20.3 | 18.8 | 39.4 | 36.7 | 35.1 | 45.2 | 52.2 | 54.6 | 14.5 | 13.3 | 14.0 | 4.9 | 5.0 | 5.1 | 0.6 | 0.6 | 0.6 | 0.52 | 0.52 | 0.51 | 0.35 | 0.40 | 0.40 |
| Southwest | 59.0 | 43.3 | 42.5 | 91.9 | 69.1 | 68.1 | 44.3 | 50.4 | 51.3 | 36.0 | 28.4 | 29.0 | 22.8 | 17.7 | 15.1 | 1.1 | 0.9 | 0.9 | 0.63 | 0.62 | 0.62 | 0.62 | 0.62 | 0.53 |
| -CY | 66.0 | 55.1 | 53.7 | 101.1 | 86.7 | 83.0 | 41.0 | 46.1 | 48.7 | 40.0 | 36.8 | 37.4 | 21.7 | 15.9 | 13.3 | 1.1 | 1.0 | 0.9 | 0.64 | 0.62 | 0.64 | 0.53 | 0.43 | 0.36 |
| -Sichuan | 67.1 | 51.4 | 50.8 | 103.6 | 81.8 | 80.7 | 45.0 | 50.9 | 52.5 | 39.9 | 31.7 | 32.0 | 21.7 | 17.1 | 15.4 | 1.0 | 0.9 | 0.9 | 0.63 | 0.62 | 0.62 | 0.54 | 0.55 | 0.49 |
| -Chongqing | 63.4 | 54.7 | 53.0 | 95.3 | 84.5 | 76.9 | 35.9 | 36.2 | 40.8 | 37.4 | 43.4 | 44.7 | 23.9 | 16.4 | 12.7 | 1.1 | 1.1 | 0.9 | 0.64 | 0.63 | 0.68 | 0.63 | 0.38 | 0.29 |
| -Guizhou | 52.5 | 32.9 | 33.5 </ | | | | | | | | | | | | | | | | | | | | | |

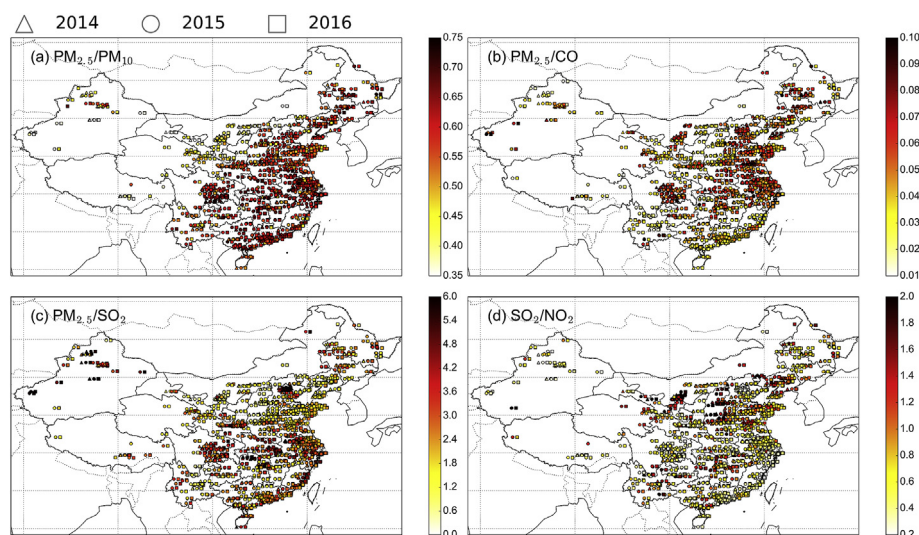


Fig. 4. Spatial distribution of the site-specific annual ratios between air pollutants (the longitude of NAQMS in 2014 and 2016 were shifted to left side (-0.7°) and right side ($+0.7^\circ$) of those in 2015, respectively).

except for PRD and the south of China. The formation rate of O_3 depends on the photochemical reactions affected by solar radiation and temperature, and precursor (NO_x and VOCs) emissions (Fu et al., 2015; Jaffe and Zhang, 2017; Lee et al., 2017; Phalitnonkiat et al., 2016; Pusede and Cohen, 2012; Pusede et al., 2014, 2015). O_3 pollution in PRD and south of China showed a steady trend in all four seasons because the temperatures are always high throughout the year in those low-latitude locations.

No obvious seasonal patterns were observed in the ratios between pollutants, except for SO_2/NO_2 . $PM_{2.5}/PM_{10}$ was slightly higher in winter than those in other seasons (Zhang and Cao, 2015). $PM_{2.5}/PM_{10}$ showed a dramatic decrease in spring (March to May) in northern China because of the high emissions of coarse particulate matter from sand and soil during the spring when it is very dry, windy, and dusty in northern China. Generally, $PM_{2.5}/PM_{10}$ was the highest in southern China throughout the year, suggesting the importance of combustion sources and secondary formation of fine particles (Zhang and Cao, 2015).

$PM_{2.5}/CO$ and $PM_{2.5}/SO_2$ were the highest in the CY mega-city cluster in winter and in the BTH mega-city cluster in summer, showing the contribution of secondary and non-industrial sources to $PM_{2.5}$. The Sichuan Basin was reported to have the highest secondary organic aerosol concentrations in China in all seasons, with hourly concentrations as high as $50 \mu g m^{-3}$ (Hu et al., 2017). The lowest SO_2/NO_2 was observed in PRD and CY and associated with vehicle emissions. SO_2/NO_2 in BTH showed a large increase during the domestic heating period (October to April) in winter. However, the peak mass ratios of SO_2 -to- NO_2 decreased dramatically during the last four years because of the full implementation of the “coal-to-natural gas” project in the entire BTH cluster. Beijing already transformed 1890-MW coal-fired boilers to natural gas-fired boilers, and currently, 2640-MW coal-fired boilers are being converted to natural gas-fired boilers. Beijing plans to remove all small coal-fired boilers in the region by the end of 2017.

The diurnal variation of hourly PWA concentrations of air pollutants were illustrated in Fig. 6, and marked with triangle in 2014, circle in 2015, and square in 2016 (filled with standard deviations), respectively. Generally, the lowest PWA concentrations of particulate matters ($PM_{2.5}$ and PM_{10}) and trace gases (NO_2 , SO_2 and CO) in China were all observed in afternoon hours (15:00–16:00 LT) when the boundary layer becomes larger and wind speed increases

(Zhang and Cao, 2015; Zhao et al., 2016). However, diurnal variations of O_3 concentrations were opposite to that of other pollutants, where the highest values were in the afternoon (14:00–15:00 LT) because of large NO_2 photolysis rates and photochemical reactions occurring at that time (Song et al., 2016). Generally, the differences of mean diurnal variations of PWA concentrations of air pollutants among the four seasons in China were small, while their amplitudes have large discrepancies with the highest O_3 concentrations in summer (attributing to the temperature-dependent atmospheric chemistry) and highest other pollutant concentrations in winter (Pusede et al., 2015; Zhao et al., 2016).

The diurnal variations of change-rates of particulate matters ($PM_{2.5}$ and PM_{10}) and trace gases (NO_2 , SO_2 and CO) all showed bimodal tendencies (Fig. 5a, b, h, j, and l), consistent with morning and evening traffic peak (Jing et al., 2016). Additionally, the diurnal variations of change-rates of particulate matters ($PM_{2.5}$ and PM_{10}) correlated best with those of CO ($r = 0.80$ for $PM_{2.5}$, $r = 0.77$ for PM_{10}), followed by SO_2 ($r = 0.78$ for $PM_{2.5}$, $r = 0.80$ for PM_{10}), and NO_2 ($r = 0.66$ for $PM_{2.5}$, $r = 0.71$ for PM_{10}), suggesting the pollutants maybe originated from identical sources such as vehicle and industrial emissions. The diurnal variations of change-rates of O_3 showed opposite tendency, comparing to its precursors NO_2 ($r = -0.75$) and CO ($r = -0.70$), indicating that the chemical process was a dominate factor in determining the O_3 diurnal variation.

The seasonal differences of the diurnal variations of change-rates of PWA concentrations were observed in China (Fig. 6), while the inter-annual differences of those were small (see Fig. 5). The change-rate of O_3 was observed to be larger in summer than in winter, especially during the daytime, suggesting that the temperature-dependent photochemical reactions were dominated factors in determining the O_3 diurnal variations in summer. In summer (winter), the highest (lowest) change-rates of O_3 were observed in 11:00–12:00 a.m. (LT) with 17.3 ± 3.8 (mean value \pm standard deviation) (8.7 ± 3.0) $\mu g m^{-3} h^{-1}$ in 2014, 16.4 ± 4.4 (7.8 ± 2.6) $\mu g m^{-3} h^{-1}$ in 2015, and 17.6 ± 5.6 (10.0 ± 3.8) $\mu g m^{-3} h^{-1}$ in 2016, respectively, suggesting the photochemical production of O_3 in winter is strongly depressed which is consistent with previous study (Liu et al., 2016a). The change-rates of $PM_{2.5}$, PM_{10} , CO, and SO_2 was observed to be larger during traffic peak in wintertime. Weilenmann et al. (2009) reported that, for gasoline cars, the majority of the CO and HC (hydrocarbon) total emissions in

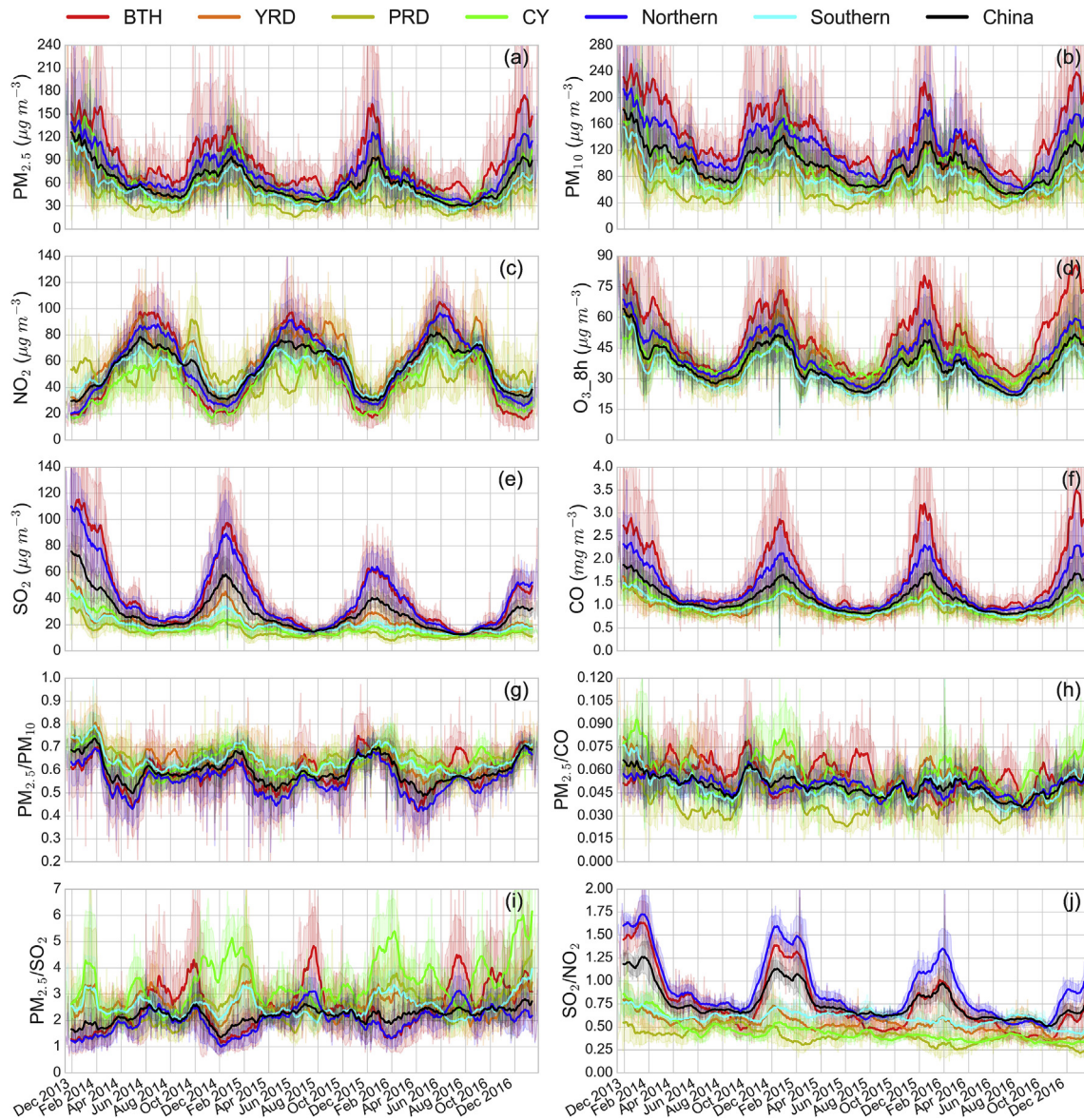


Fig. 5. Three-year time series of PWA mass concentrations and ratios in Chinese megacity clusters (BTH, YRD, PRD, and CY), and the northern and southern China. (The solid lines were monthly moving average concentrations, filled with monthly moving standard deviations).

average real-world driving are due to cold-start extra emissions, whereas the particle and NO_x emission of cold starts are less significant. The larger change-rates of PM during traffic peak in wintertime are likely due to high secondary formation in aerosol water in wintertime (see Fig. 6). Gentner et al. (2012) reported that diesel and gasoline vehicle emissions are important for air quality, and 65%–90% of the vehicular-derived secondary aerosol are estimated from diesel exhaust. With the further emissions control, the contribution to aerosol for direct emissions may decrease, and secondary aerosol contribution should attract more attention.

3.4. The major pollutant and non-attainment days

The days that each criteria pollutant was designated as a “major pollutant” were recorded in 31 provinces and seven regions (Fig. 7 and Table S9). In this study, “O₃” represent either O_{3_8h} or O_{3_1h}. The provinces and regions in Fig. 7 are ranked by the number of days of no “major pollutants” (AQI < 50, excellent air quality) in

2016. Based on this ranking, the five most polluted provinces were Xinjiang (0 days), Shandong (10 days), Henan (12 days), Hebei (15 days), and Ningxia (16 days). The five provinces with best air quality were Hainan (297 days), Fujian (204 days), Yunnan (193 days), Guangdong (186 days), and Guangxi (168 days). The most polluted megacity clusters were BTH (25 days), followed by CY (58), YRD (62 days), and PRD (153 days). At the geographic regions-level, the most polluted region was the northwest (2 days), followed by the north (12 days), central (28 days), east (76 days), northeast (87 days), southwest (88 days), and south (188 days). From the inter-annual perspective, the number of days with AQI < 50 increased in all Chinese provinces except Xinjiang province in three years (7 days in 2014, 2 days in 2015, 0 days in 2016). Although the Ministry of Environmental Protection has loosened the air quality classification (breakpoints) standards for each air pollutant compared to the AQI system (EPA-454/B-16-002) of the U.S. Environmental Protection Agency, the AQI values calculated with PWA daily concentrations of air pollutants in China were still very high with only a

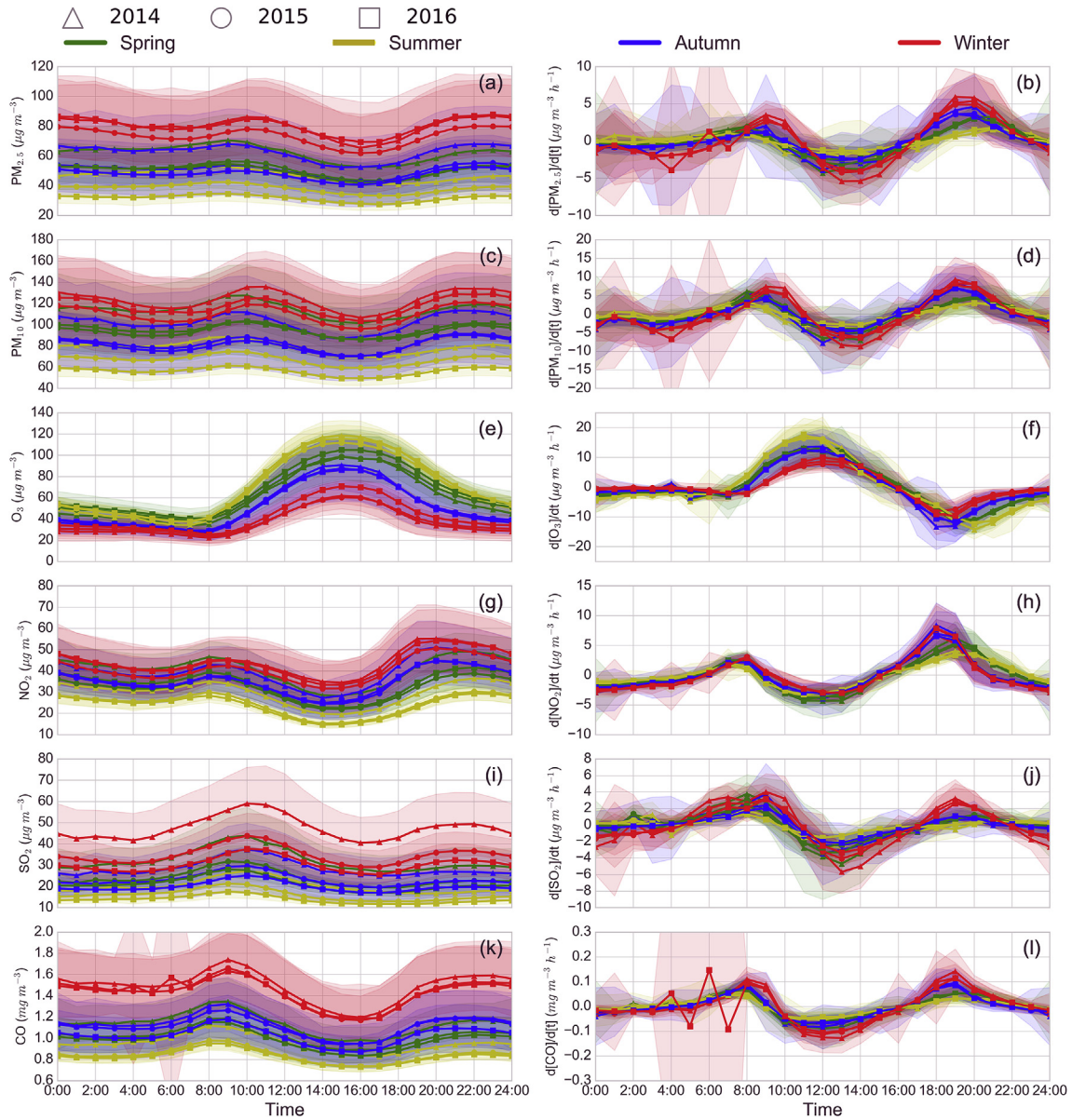


Fig. 6. The diurnal variations and change-rates of air pollutants during different seasons in China (Solid line represents hourly average concentrations, filled with hourly standard deviations).

few days (one day in 2014, four days in 2015, and seventeen days in 2016) of excellent air quality.

PM_{2.5} was the pollutant most frequently designated as a major pollutant in most regions (north: 163 d, southwest: 151 d, central: 150 d, east: 140 d, northeast: 124 d, south: 92 d) except for the northwest of China (93 d). PM₁₀ was the one most frequently designated as a major pollutant in the northwest region. The Gobi Desert and other deserts, located in the northwest region of China, are the major sources of sandstorms and dust constituting particulate matters (He et al., 2017; Zhao et al., 2016). In 2016, O₃ emerged as the second frequent major pollutant in central (106 d), north (104 days), and south (63 d) regions. However, in 2014, PM₁₀ was the second frequent major pollutant in all regions except for the south region. In 2016, O₃ was the most frequent major pollutant in YRD (118 d) and PRD (98 days), and PM_{2.5} was most frequent major pollutant in BTH (178 d) and CY (189 d). Overall, the most frequent major pollutant in the whole country was PM_{2.5} (134 d), followed

by PM₁₀ (128 d) and O₃ (87 d). The occurrences of CO, NO₂, and SO₂ as major pollutants were considerably less frequent compared to PM and O₃. The complex mixture of PM and O₃ threatens the health of a large portion of the Chinese population.

The non-attainment days of each air pollutants were not equally distributed throughout the year because of the seasonal variations of the concentrations of each air pollutant (Cheng et al., 2016b). Fig. 8 and Table S10 show the monthly distribution of the non-attainment days of each pollutant in each province and region across China for the three years. November, December and January were the dominant months of non-attainment days for all of regions, primarily in southwest, central, northwest and north regions, except during the summertime in Beijing. For non-attainment days of PM_{2.5}, winter months had the largest number of polluted days in each region, consistent with previous studies (Cheng et al., 2016b; Wang et al., 2014b). Combination of coal combustion and biomass burning for residential heating, and stagnant meteorological

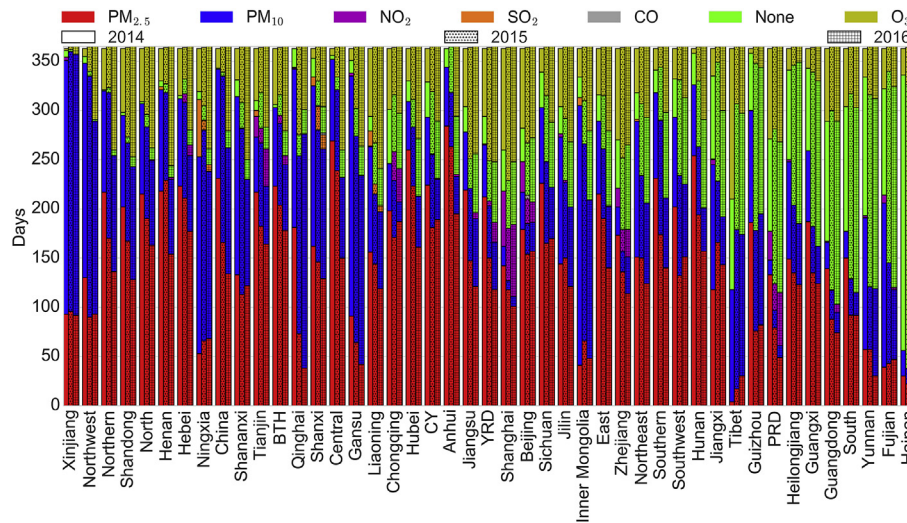


Fig. 7. The number days in every year with major pollutants. (The provinces and regions are ranked sorted by the number of days of no “major pollutants” (AQI<50, excellent air quality) in 2016; the three histograms in each province or region represent, from left to right in order, year 2014, 2015, and 2016, respectively).

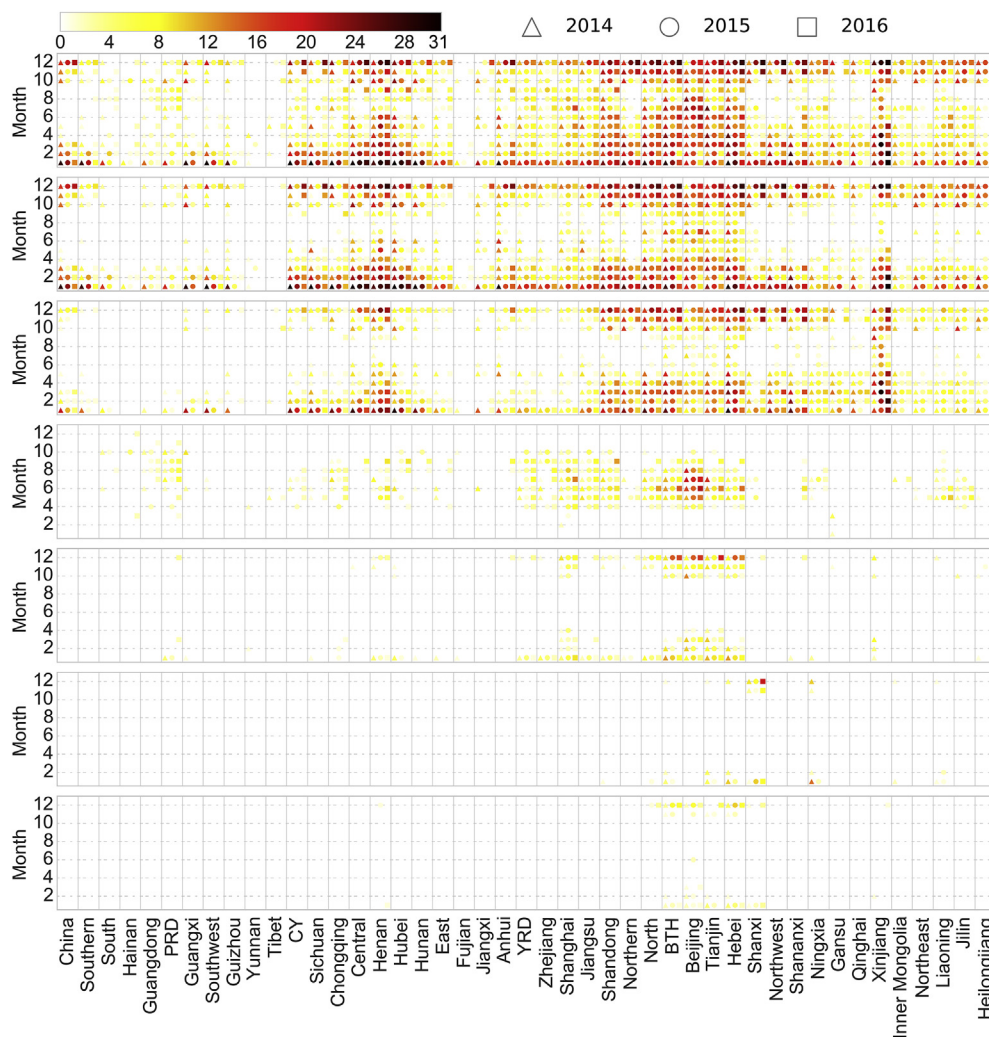


Fig. 8. The monthly distribution for the non-attainment days for each pollutant (from upper to bottom: AQI, PM_{2.5}, PM₁₀, O₃, NO₂, SO₂ and CO) during the three-year period. The colors represent the number of the non-attainment days. (For interpretation of the references to colour in this figure legend, the reader is referred to the web version of this article.)

conditions (vertical temperature inversion and low boundary layer height) were responsible for the peak PM_{2.5} season (He et al., 2016a; Huang et al., 2014b; Liu et al., 2017; Sun et al., 2014; Yang et al., 2016). From the inter-annual perspective, the number of polluted days with PM_{2.5} concentrations over 75 $\mu\text{g m}^{-3}$ increased in BTH in winter, especially in November and December owing to the weakening of the East Asian winter monsoon because of the climate change (Ogata et al., 2014; Xu et al., 2016). Strong relationships between foggy-hazy days and the intensity of the East Asian winter monsoon were reported to elucidate the aerosol pollution in winter over East Asia (Jeong and Park, 2017; Li et al., 2016a). The monthly distribution of the polluted days with PM₁₀ > 150 $\mu\text{g m}^{-3}$ is correlated ($r = 0.85$, $p < 0.001$) with the days with PM_{2.5} > 100 $\mu\text{g m}^{-3}$ (Fig. S6). Summer is the O₃ episode season in Chinese mega-city clusters, especially in BTH and YRD (Fig. 8) (Ran et al., 2012; Song et al., 2016; Wang et al., 2017b; Zhao et al., 2009). The O₃ CAAQS exceedance probability in BTH was highest in June (15 d), followed by May (10 d), and July (7 d). Summertime ozone pollution in Beijing is much more severe than in the other regions since the highest O₃ CAAQS exceedance probabilities were reported in Beijing (Fig. 8). Previous studies suggested that the oxidation of VOCs (especially aromatics) and heterogeneous reactions (e.g. HONO formation and aerosol update HO₂) play potentially critical roles in O₃ production in Beijing (Liu et al., 2012; Shao et al., 2009; Zhang et al., 2014b). The polluted days with NO₂ > 100 $\mu\text{g m}^{-3}$ were mainly observed in BTH and YRD during the winter season. Shanxi, Hebei, and Ningxia are the three provinces with a few days of SO₂ > 150 $\mu\text{g m}^{-3}$. In Ningxia province, high SO₂ pollution was recorded in 28 d in 2014, 2 d in 2015, and 0 d in 2016. The environmental effects of stringent SO₂ emission regulations in Ningxia were clearly observed in this study (van der A et al., 2017). However, in Shanxi province, non-attainment days of SO₂ was recorded in 13 d in 2014, 18 d in 2015, and 35 d in 2016. The non-attainment days of SO₂ was as high as 20 d in Shanxi province in December 2016. Additionally, annual PWA concentrations of SO₂ in Shanxi province (56.5 $\mu\text{g m}^{-3}$ in 2014, 59.6 $\mu\text{g m}^{-3}$ in 2015, and 65.2 $\mu\text{g m}^{-3}$ in 2016) were 65.7%, 129.2%, and 197.7% higher than the national average in 2014, 2015, and 2016, respectively. According to the Environmental Protection Agency of Linfen (one of the most SO₂ polluted cities in Shanxi province, with an annual concentration of 82.8 $\mu\text{g m}^{-3}$ in 2016), 70% of coal combustion-related SO₂ emissions in the city are from the residential combustion of solid biomass and coal for cooking and heating in winter. Severe SO₂ pollution and its health impacts in Shanxi province during wintertime need further investigation. Polluted days with CO > 4 mg m⁻³ were mainly distributed in the north region (including the BTH mega-city cluster and Shanxi province) during the winter season.

3.5. Correlations between air pollutants

Figs. S7 and S8 show the distribution of data and correlations between the annual average concentrations of pollutants at each NAQMS in megacity clusters and seven geographic regions, respectively. The Pearson's correlation coefficients (r) in Figs. S7 and S8 are calculated as shown in Tables S11 and S12. Over the three-year period, PM_{2.5} concentrations were strongly correlated ($r > 0.8$) with PM₁₀ in all mega-city clusters and geographic regions. Annual mass concentrations of PM_{2.5} and PM₁₀ were positively correlated with NO₂, SO₂, and CO in mega-city clusters, suggesting that the common source of these species was fossil fuel combustion. However, annual mass concentrations of PM (including PM_{2.5} and PM₁₀) were weakly correlated with SO₂ in the northwest (PM_{2.5}: $r = 0.20$, PM₁₀: $r = 0.05$) and southwest (PM_{2.5}: $r = 0.16$, PM₁₀: $r = 0.14$), highlighting relative low contributions of coal

combustion to PM in the northwest and southwest regions. O₃ is significantly ($p < 0.05$) negatively correlated with its precursors (such as NO₂ and CO) and PM in mega-city clusters and the northern China. To further investigate the relative contribution of SO₂ and NO₂ to PM_{2.5} across China, a multiple linear regression analysis (annual PM_{2.5} concentrations as a function of SO₂ and NO₂) was conducted in each mega-city cluster and region (Table S13). The coefficients of NO₂ were 150.5%, 203.2%, 144.9%, 627.0%, 34.6%, 565.5%, 418.9%, and 113.3% higher than those of SO₂, in BTH, north, northeast, northwest, central, and southwest of China, respectively. This finding implies that NO_x controls in those regions are more beneficial than SO₂ controls for the improvement of PM air quality. Previous studies also indicated that reactive nitrogen chemistry in aerosol water can explain the missing source of sulfate in the North China Plain during winter haze episodes (Cheng et al., 2016a). Additionally, the regression parameters for SO₂ are 68.0%, 70.5%, 24.0%, 79.5%, 27.6%, and 10.8% higher than those for NO₂, in YRD, PRD, CY, South, East, and Southern, respectively. This finding implies that SO₂ controls in those regions, mostly in the Southern China, are more beneficial than NO_x controls to the improvement of PM air quality. However, the emission characteristics, climate and topographic systems across China were different and complex, and rapid air pollution episodes are often associated with regional transport (Hu et al., 2015; Li et al., 2017; Ming et al., 2017; Sun et al., 2014; Xue et al., 2014; Zheng et al., 2015), the relationship between air pollution associating with meteorological conditions and secondary formation need further investigation.

4. Conclusions

This study analyzed air quality monitoring data and presented the current status of air pollution in China from January 2014 to December 2016. The population exposure, spatial and temporal variations of air pollutants (PM_{2.5}, PM₁₀, O₃, NO₂, SO₂, and CO), the major pollutants, the temporal evolution of polluted days, and inter-correlation of air pollutants were investigated. Based on the three-year data from the NAQMS network, the overall status of China's air pollution problem is presented. In 2014 (2015, 2016), annual population-weighted-average (PWA) values in China were 65.8 (55.0, 50.7) $\mu\text{g m}^{-3}$ for PM_{2.5}, 107.8 (91.1, 85.7) $\mu\text{g m}^{-3}$ for PM₁₀, 54.8 (56.2, 57.2) $\mu\text{g m}^{-3}$ for O₃-8 h, 39.6 (33.3, 33.4) $\mu\text{g m}^{-3}$ for NO₂, 34.1 (26, 21.9) $\mu\text{g m}^{-3}$ for SO₂, 1.2 (1.1, 1.1) mg m⁻³ for CO, and 0.60 (0.59, 0.58) for PM_{2.5}/PM₁₀, respectively. In 2014 (2015, 2016), 7% (14%, 19%), 17% (27%, 34%), 51% (67%, 70%) and 88% (97%, 98%) of the population in China lived in areas that meet the level of annual PM_{2.5}, PM₁₀, NO₂, and SO₂ standard metrics from Chinese Ambient Air Quality Standards-Grade II. The annual PWA concentrations of PM_{2.5}, PM₁₀, O₃-8 h, NO₂, SO₂, CO in the Northern China are about 40.4%, 58.9%, 5.9%, 24.6%, 96.7%, and 38.1% higher than those in Southern China, respectively. Though the air quality has been improving recent years, PM_{2.5} pollution in wintertime is worsening, especially in the Northern China. The most frequent major pollutant in China is PM_{2.5} (231 days in 2014, 166 days in 2015, 134 days in 2016), followed by PM₁₀ (111, 169, 128 days) and O₃ (20, 26, 87 days). No significant patterns were detected for annual average O₃ concentrations because of its complex, nonlinear, and temperature-dependent chemistry. O₃ formation and control strategies in China need further investigation.

Changes in monthly moving average concentrations of PM (including PM_{2.5} and PM₁₀), NO₂, SO₂, and CO conformed to U-shaped patterns with the highest values in winter (December to February) and the lowest in summer (June to August). The 8-h O₃ values in all regions exhibited mountain-peak-shaped patterns (opposite to the U-shaped patterns) with the highest concentrations in summer and the lowest in winter, except for PRD and the

south of China. Based on the daily PWA concentrations of air pollutants, the most frequent major pollutant in China is PM_{2.5} (231 days in 2014, 166 days in 2015, 134 days in 2016), followed by PM₁₀ (111, 169, 128 days) and O₃ (20, 26, 87 days). The complex mixture of PM and O₃ pollution is an emerging problem threatening a large portion of the Chinese population, especially in Chinese mega-city clusters. Based on the results of the multiple linear regression analysis (annual PM_{2.5} concentrations as a function of SO₂ and NO₂), NO_x controls were more beneficial than SO₂ controls for improvement of PM air quality in the northern China, central, and southwest regions. On the other hand, SO₂ controls were more beneficial than NO_x controls mostly in southern China (including YRD, PRD, CY, south, and east). The results of the study should be interpreted with caution since the analyses were carried out using annual average mass concentrations, not the single pollution episodes. We urge public health researchers to conduct environmental health assessments using the results of this study.

Acknowledgements

This work was supported by the National Science and Technology Infrastructure Program (2014BAC23B02), the Special Scientific Research Funds for National Basic Research Program of China (2013FY112700-05). The author declare they have no competing financial interests. We are very grateful to the China National Environmental Monitoring Center (<http://113.108.142.147:20035/emcpublish/>) for the provision of three-year air quality monitoring data used in this study. The constructive suggestions from the anonymous reviewers are greatly appreciated. The authors declare that they have no competing financial interests.

Appendix A. Supplementary data

Supplementary data related to this article can be found at <http://dx.doi.org/10.1016/j.envpol.2017.04.075>.

References

- Aneja, V.P., Agarwal, A., Roelle, P.A., Phillips, S.B., Tong, Q., Watkins, N., Yablonsky, R., 2001. Measurements and analysis of criteria pollutants in New Delhi, India. *Environ. Int.* 27, 35–42.
- Barrero, M.A., Orza, J.A., Cabello, M., Canton, L., 2015. Categorisation of air quality monitoring stations by evaluation of PM(10) variability. *Sci. Total Environ.* 524–525, 225–236.
- Cao, J., Yang, C., Li, J., Chen, R., Chen, B., Gu, D., Kan, H., 2011. Association between long-term exposure to outdoor air pollution and mortality in China: a cohort study. *J. Hazard Mater.* 186, 1594–1600.
- Chai, F., Gao, J., Chen, Z., Wang, S., Zhang, Y., Zhang, J., Zhang, H., Yun, Y., Ren, C., 2014. Spatial and temporal variation of particulate matter and gaseous pollutants in 26 cities in China. *J. Environ. Sci.* 26, 75–82.
- Chen, X., Zhang, L.W., Huang, J.J., Song, F.J., Zhang, L.P., Qian, Z.M., Trevathan, E., Mao, H.J., Han, B., Vaughn, M., Chen, K.X., Liu, Y.M., Chen, J., Zhao, B.X., Jiang, G.H., Gu, Q., Bai, Z.P., Dong, G.H., Tang, N.J., 2016. Long-term exposure to urban air pollution and lung cancer mortality: a 12-year cohort study in Northern China. *Sci. Total Environ.* 571, 855–861.
- Chen, Y., Ebenstein, A., Greenstone, M., Li, H., 2013. Evidence on the impact of sustained exposure to air pollution on life expectancy from China's Huai River policy. *Proc. Natl. Acad. Sci.* 110, 12936–12941.
- Cheng, Y., Zheng, G., Wei, C., Mu, Q., Zheng, B., Wang, Z., Gao, M., Zhang, Q., He, K., Carmichael, G., Pöschl, U., Su, H., 2016a. Reactive nitrogen chemistry in aerosol water as a source of sulfate during haze events in China. *Sci. Adv.* 2.
- Cheng, Z., Luo, L., Wang, S., Wang, Y., Sharma, S., Shimadera, H., Wang, X., Bressi, M., de Miranda, R.M., Jiang, J., Zhou, W., Fajardo, O., Yan, N., Hao, J., 2016b. Status and characteristics of ambient PM_{2.5} pollution in global megacities. *Environ. Int.* 89–90, 212–221.
- Clapp, L.J., Jenkin, M.E., 2001. Analysis of the relationship between ambient levels of O₃, NO₂ and NO as a function of NO_x in the UK. *Atmos. Environ.* 35, 6391–6405.
- Dockery, D.W., Pope, C.A., Xu, X., Spengler, J.D., Ware, J.H., Fay, M.E., Ferris Jr., B.G., Speizer, F.E., 1993. An association between air pollution and mortality in six US cities. *N. Engl. J. Med.* 329, 1753–1759.
- Forouzanfar, M.H., Afshin, A., Alexander, L.T., Anderson, H.R., Bhutta, Z.A., 2016. Global, regional, and national comparative risk assessment of 79 behavioural, environmental and occupational, and metabolic risks or clusters of risks, 1990–2015: a systematic analysis for the Global Burden of Disease Study 2015. *Lancet* 388, 1659–1724.
- Fu, T.M., Zheng, Y., Paulot, F., Mao, J., Yantosca, R.M., 2015. Positive but variable sensitivity of August surface ozone to large-scale warming in the southeast United States. *Nat. Clim. Change* 5, 454–458.
- Gentner, D.R., Isaacman, G., Worton, D.R., Chan, A.W.H., Dallmann, T.R., Davis, L., Liu, S., Day, D.A., Russell, L.M., Wilson, K.R., Weber, R., Guha, A., Harley, R.A., Goldstein, A.H., 2012. Elucidating secondary organic aerosol from diesel and gasoline vehicles through detailed characterization of organic carbon emissions. *Proc. Natl. Acad. Sci.* 109, 18318–18323.
- Guan, W.-J., Zheng, X.-Y., Chung, K.F., Zhong, N.-S., 2016. Impact of air pollution on the burden of chronic respiratory diseases in China: time for urgent action. *Lancet* 388, 1939–1951.
- Guo, S., Hu, M., Zamora, M.L., Peng, J., Shang, D., Zheng, J., Du, Z., Wu, Z., Shao, M., Zeng, L., Molina, M.J., Zhang, R., 2014. Elucidating severe urban haze formation in China. *Proc. Natl. Acad. Sci. U. S. A.* 111, 17373–17378.
- Harrison, R.M., Dall'Osto, M., Beddows, D.C.S., Thorpe, A.J., Bloss, W.J., Allan, J.D., Coe, H., Dorsey, J.R., Gallagher, M., Martin, C., Whitehead, J., Williams, P.I., Jones, R.L., Langridge, J.M., Benton, A.K., Ball, S.M., Langford, B., Hewitt, C.N., Davison, B., Martin, D., Petersson, K.F., Henshaw, S.J., White, I.R., Shallcross, D.E., Barlow, J.F., Dunbar, T., Davies, F., Nemitz, E., Phillips, G.J., Helfter, C., Di Marco, C.F., Smith, S., 2012. Atmospheric chemistry and physics in the atmosphere of a developed megacity (London): an overview of the REPARTEE experiment and its conclusions. *Atmos. Chem. Phys.* 12, 3065–3114.
- He, J., Gong, S., Yu, Y., Yu, L., Wu, L., Mao, H., Song, C., Zhao, S., Liu, H., Li, X., Li, R., 2017. Air pollution characteristics and their relation to meteorological conditions during 2014–2015 in major Chinese cities. *Environ. Pollut.* 223, 484–496.
- He, J., Wu, L., Mao, H., Li, R., 2016a. Impacts of meteorological conditions on air quality in urban Langfang, Hebei Province. *Res. Environ. Sci.* 29, 791–799.
- He, J., Wu, L., Mao, H., Liu, H., Jing, B., Yu, Y., Ren, P., Feng, C., Liu, X., 2016b. Development of a vehicle emission inventory with high temporal–spatial resolution based on NRT traffic data and its impact on air pollution in Beijing – Part 2: impact of vehicle emission on urban air quality. *Atmos. Chem. Phys.* 16, 3171–3184.
- Hu, J., Wang, P., Ying, Q., Zhang, H., Chen, J., Ge, X., Li, X., Jiang, J., Wang, S., Zhang, J., Zhao, Y., Zhang, Y., 2017. Modeling biogenic and anthropogenic secondary organic aerosol in China. *Atmos. Chem. Phys.* 17, 77–92.
- Hu, J., Wang, Y., Ying, Q., Zhang, H., 2014. Spatial and temporal variability of PM_{2.5} and PM₁₀ over The north China plain and the Yangtze River Delta, China. *Atmos. Environ.* 95, 598–609.
- Hu, J., Wu, L., Zheng, B., Zhang, Q., He, K., Chang, Q., Li, X., Yang, F., Ying, Q., Zhang, H., 2015. Source contributions and regional transport of primary particulate matter in China. *Environ. Pollut.* 207, 31–42.
- Huang, R.J., Zhang, Y., Bozzetti, C., Ho, K.F., Cao, J.J., Han, Y., Daellenbach, K.R., Slowik, J.G., Platt, S.M., Canonaco, F., Zotter, P., Wolf, R., Pieber, S.M., Bruns, E.A., Crippa, M., Ciarelli, G., Piazzalunga, A., Schwikowski, M., Abbaszade, G., Schnelle-Kreis, J., Zimmermann, R., An, Z., Szidat, S., Baltensperger, U., El Haddad, I., Prevot, A.S., 2014a. High secondary aerosol contribution to particulate pollution during haze events in China. *Nature* 514, 218–222.
- Huang, Y., Shen, H., Chen, H., Wang, R., Zhang, Y., Su, S., Chen, Y., Lin, N., Zhuo, S., Zhong, Q., Wang, X., Liu, J., Li, B., Liu, W., Tao, S., 2014b. Quantification of global primary emissions of PM_{2.5}, PM₁₀, and TSP from combustion and industrial process sources. *Environ. Sci. Technol.* 48, 13834–13843.
- Jaffe, D.A., Zhang, L., 2017. Meteorological anomalies lead to elevated O₃ in the western U.S. in June 2015. *Geophys. Res. Lett.* 44, 2016GL072010.
- Jeong, J.I., Park, R.J., 2017. Winter monsoon variability and its impact on aerosol concentrations in East Asia. *Environ. Pollut.* 221, 285–292.
- Jing, B., Wu, L., Mao, H., Gong, S., He, J., Zou, C., Song, G., Li, X., Wu, Z., 2016. Development of a vehicle emission inventory with high temporal–spatial resolution based on NRT traffic data and its impact on air pollution in Beijing – Part 1: development and evaluation of vehicle emission inventory. *Atmos. Chem. Phys.* 16, 3161–3170.
- Kampa, M., Castanas, E., 2008. Human health effects of air pollution. *Environ. Pollut.* 151, 362–367.
- Kan, H., Chen, R., Tong, S., 2012. Ambient air pollution, climate change, and population health in China. *Environ. Int.* 42, 10–19.
- Landrigan, P.J., 2016. Air Pollution and Health. *The Lancet Public Health*.
- Lee, Y.C., Shindell, D.T., Faluvegi, G., Wenig, M., Lam, Y.F., Ning, Z., Hao, S., Lai, C.S., 2017. Increase of ozone concentrations, its temperature sensitivity and the precursor factor in South China. *Tellus B Chem. Phys. Meteorology* 66, 23455.
- Lepeule, J., Laden, F., Dockery, D., Schwartz, J., 2012. Chronic exposure to fine particles and mortality: an extended follow-up of the Harvard Six Cities study from 1974 to 2009. *Environ. Health Perspect.* 120, 965–970.
- Li, J., Du, H., Wang, Z., Sun, Y., Yang, W., Li, J., Tang, X., Fu, P., 2017. Rapid formation of a severe regional winter haze episode over a mega-city cluster on the North China Plain. *Environ. Pollut.* 223, 605–615.
- Li, Q., Zhang, R., Wang, Y., 2016a. Interannual variation of the wintertime fog-haze days across central and eastern China and its relation with East Asian winter monsoon. *Int. J. Climatol.* 36, 346–354.
- Li, R., Mao, H., Wu, L., He, J., Ren, P., Li, X., 2016b. The evaluation of emission control to PM concentration during Beijing APEC in 2014. *Atmos. Pollut. Res.* 7, 363–369.
- Li, S., Williams, G., Guo, Y., 2016c. Health benefits from improved outdoor air quality and intervention in China. *Environ. Pollut.* 214, 17–25.
- Liu, B., Liang, D., Yang, J., Dai, Q., Bi, X., Feng, Y., Yuan, J., Xiao, Z., Zhang, Y., Xu, H.,

- 2016a. Characterization and source apportionment of volatile organic compounds based on 1-year of observational data in Tianjin, China. *Environ. Pollut.* 218, 757–769.
- Liu, F., Zhang, Q., van der A, R.J., Zheng, B., Tong, D., Yan, L., Zheng, Y., He, K., 2016b. Recent reduction in NO_x emissions over China: synthesis of satellite observations and emission inventories. *Environ. Res. Lett.* 11, 114002.
- Liu, T., Gong, S., He, J., Yu, M., Wang, Q., Li, H., Liu, W., Zhang, J., Li, L., Wang, X., Li, S., Lu, Y., Du, H., Wang, Y., Zhou, C., Liu, H., Zhao, Q., 2017. Attributions of meteorological and emission factors to the 2015 winter severe haze pollution episodes in China's Jing-Jin-Ji area. *Atmos. Chem. Phys.* 17, 2971–2980.
- Liu, Z., Wang, Y., Gu, D., Zhao, C., Huey, L.G., Stickel, R., Liao, J., Shao, M., Zhu, T., Zeng, L., Amoroso, A., Costabile, F., Chang, C.C., Liu, S.C., 2012. Summertime photochemistry during CAREBeijing-2007: RO_x budgets and O₃ formation. *Atmos. Chem. Phys.* 12, 7737–7752.
- Mao, X., Zhou, J., Corsetti, G., 2014. How well have China's recent five-year plans been implemented for energy conservation and air pollution control? *Environ. Sci. Technol.* 48, 10036–10044.
- MEP, 2012. Technical Regulation on Ambient Air Quality Index (On Trial) (HJ 633–2012).
- Ming, L., Jin, L., Li, J., Fu, P., Yang, W., Liu, D., Zhang, G., Wang, Z., Li, X., 2017. PM_{2.5} in the Yangtze River Delta, China: chemical compositions, seasonal variations, and regional pollution events. *Environ. Pollut.* 223, 200–212.
- Nirel, R., Dayan, U., 2001. On the ratio of sulfur dioxide to nitrogen oxides as an indicator of air pollution sources. *J. Appl. Meteorology* 40, 1209–1222.
- Ogata, T., Ueda, H., Inoue, T., Hayasaki, M., Yoshida, A., Watanabe, S., Kira, M., Ooshiro, M., Kumai, A., 2014. Projected future changes in the Asian monsoon: a comparison of CMIP3 and CMIP5 model results. *J. Meteorological Soc. Jpn. Ser. II* 92, 207–225.
- Phalitnonkiat, P., Sun, W., Grigoriu, M.D., Hess, P., Samorodnitsky, G., 2016. Extreme ozone events: tail behavior of the surface ozone distribution over the U.S. *Atmos. Environ.* 128, 134–146.
- Pusede, S.E., Cohen, R.C., 2012. On the observed response of ozone to NO_x and VOC reactivity reductions in San Joaquin Valley California 1995–present. *Atmos. Chem. Phys.* 12, 8323–8339.
- Pusede, S.E., Gentner, D.R., Wooldridge, P.J., Browne, E.C., Rollins, A.W., Min, K.E., Russell, A.R., Thomas, J., Zhang, L., Brune, W.H., Henry, S.B., DiGangi, J.P., Keutsch, F.N., Harrold, S.A., Thornton, J.A., Beaver, M.R., St Clair, J.M., Wennberg, P.O., Sanders, J., Ren, X., VandenBoer, T.C., Markovic, M.Z., Guha, A., Weber, R., Goldstein, A.H., Cohen, R.C., 2014. On the temperature dependence of organic reactivity, nitrogen oxides, ozone production, and the impact of emission controls in San Joaquin Valley, California. *Atmos. Chem. Phys.* 14, 3373–3395.
- Pusede, S.E., Steiner, A.L., Cohen, R.C., 2015. Temperature and recent trends in the chemistry of continental surface ozone. *Chem. Rev.* 115, 3898–3918.
- Ran, L., Zhao, C.S., Xu, W.Y., Han, M., Lu, X.Q., Han, S.Q., Lin, W.L., Xu, X.B., Gao, W., Yu, Q., Geng, F.H., Ma, N., Deng, Z.Z., Chen, J., 2012. Ozone production in summer in the megacities of Tianjin and Shanghai, China: a comparative study. *Atmos. Chem. Phys.* 12, 7531–7542.
- Sawvel, E.J., Willis, R., West, R.R., Casuccio, G.S., Norris, G., Kumar, N., Hammond, D., Peters, T.M., 2015. Passive sampling to capture the spatial variability of coarse particles by composition in Cleveland, OH. *Atmos. Environ.* 105, 61–69.
- Shao, M., Lu, S., Liu, Y., Xie, X., Chang, C., Huang, S., Chen, Z., 2009. Volatile organic compounds measured in summer in Beijing and their role in ground-level ozone formation. *J. Geophys. Res.* 114.
- Song, C., He, J., Wu, L., Jin, T., Chen, X., Li, R., Ren, P., Zhang, L., Mao, H., 2017. Health burden attributable to ambient PM_{2.5} in China. *Environ. Pollut.* 223, 575–586.
- Song, C.B., Li, R.P., He, J.J., Wu, L., Mao, H.J., 2016. Analysis of pollution characteristics of NO, NO₂ and O₃ at urban area of Langfang, Hebei. *Zhongguo Huanjing Kexue/China Environ. Sci.* 36, 2903–2912.
- Sun, Y., Jiang, Q., Wang, Z., Fu, P., Li, J., Yang, T., Yin, Y., 2014. Investigation of the sources and evolution processes of severe haze pollution in Beijing in January 2013. *J. Geophys. Res. Atmos.* 119, 4380–4398.
- van der A, R.J., Mijling, B., Ding, J., Koukouli, M.E., Liu, F., Li, Q., Mao, H., Theys, N., 2017. Cleaning up the air: effectiveness of air quality policy for SO₂ and NO₂ emissions in China. *Atmos. Chem. Phys.* 17, 1775–1789.
- Wang, G., Zhang, R., Gomez, M.E., Yang, L., Levy Zamora, M., Hu, M., Lin, Y., Peng, J., Guo, S., Meng, J., Li, J., Cheng, C., Hu, T., Ren, Y., Wang, Y., Gao, J., Cao, J., An, Z., Zhou, W., Li, G., Wang, J., Tian, P., Marrero-Ortiz, W., Secret, J., Du, Z., Zheng, J., Shang, D., Zeng, L., Shao, M., Wang, W., Huang, Y., Wang, Y., Zhu, Y., Li, Y., Hu, J., Pan, B., Cai, L., Cheng, Y., Ji, Y., Zhang, F., Rosenfeld, D., Liss, P.S., Duce, R.A., Kolb, C.E., Molina, M.J., 2016. Persistent sulfate formation from London Fog to Chinese haze. *Proc. Natl. Acad. Sci. U. S. A.* 113, 13630–13635.
- Wang, J., Wang, S., Jiang, J., Ding, A., Zheng, M., Zhao, B., Wong, D.C., Zhou, W., Zheng, G., Wang, L., Pleim, J.E., Hao, J., 2014a. Impact of aerosol–meteorology interactions on fine particle pollution during China's severe haze episode in January 2013. *Environ. Res. Lett.* 9, 094002.
- Wang, S., Zhou, C., Wang, Z., Feng, K., Hubacek, K., 2017a. The characteristics and drivers of fine particulate matter (PM_{2.5}) distribution in China. *J. Clean. Prod.* 142, 1800–1809.
- Wang, T., Xue, L., Brimblecombe, P., Lam, Y.F., Li, L., Zhang, L., 2017b. Ozone pollution in China: a review of concentrations, meteorological influences, chemical precursors, and effects. *Sci. Total Environ.* 575, 1582–1596.
- Wang, Y., Ying, Q., Hu, J., Zhang, H., 2014b. Spatial and temporal variations of six criteria air pollutants in 31 provincial capital cities in China during 2013–2014. *Environ. Int.* 73, 413–422.
- Weilenmann, M., Favez, J.-Y., Alvarez, R., 2009. Cold-start emissions of modern passenger cars at different low ambient temperatures and their evolution over vehicle legislation categories. *Atmos. Environ.* 43, 2419–2429.
- West, J.J., Cohen, A., Dentener, F., Brunekreef, B., Zhu, T., Armstrong, B., Bell, M.L., Brauer, M., Carmichael, G., Costa, D.L., Dockery, D.W., Kleeman, M., Krzyzanowski, M., Kunzli, N., Liousse, C., Lung, S.C., Martin, R.V., Poschl, U., Pope 3rd, C.A., Roberts, J.M., Russell, A.G., Wiedinmyer, C., 2016. What we breathe impacts our health: improving understanding of the link between air pollution and health. *Environ. Sci. Technol.* 50, 4895–4904.
- Wongphatarakul, V., Friedlander, S.K., Pinto, J.P., 1998. A comparative study of PM_{2.5} ambient aerosol chemical databases. *Environ. Sci. Technol.* 32, 3926–3934.
- Wu, Y., Zhang, S., Hao, J., Liu, H., Wu, X., Hu, J., Walsh, M.P., Wallington, T.J., Zhang, K.M., Stevanovic, S., 2017. On-road vehicle emissions and their control in China: a review and outlook. *Sci. Total Environ.* 574, 332–349.
- Xie, Y., Dai, H., Dong, H., Hanaoka, T., Masui, T., 2016. Economic impacts from PM_{2.5} pollution-related health effects in China: a provincial-level analysis. *Environ. Sci. Technol.* 50, 4836–4843.
- Xu, H., Bi, X.H., Zheng, W.W., Wu, J.H., Feng, Y.C., 2015. Particulate matter mass and chemical component concentrations over four Chinese cities along the western Pacific coast. *Environ. Sci. Pollut. Res. Int.* 22, 1940–1953.
- Xu, M., Xu, H., Ma, J., 2016. Responses of the East Asian winter monsoon to global warming in CMIP5 models. *Int. J. Climatol.* 36, 2139–2155.
- Xue, L.K., Wang, T., Gao, J., Ding, A.J., Zhou, X.H., Blake, D.R., Wang, X.F., Saunders, S.M., Fan, S.J., Zuo, H.C., Zhang, Q.Z., Wang, W.X., 2014. Ground-level ozone in four Chinese cities: precursors, regional transport and heterogeneous processes. *Atmos. Chem. Phys.* 14, 13175–13188.
- Yang, Y.Q., Wang, J.Z., Gong, S.L., Zhang, X.Y., Wang, H., Wang, Y.Q., Wang, J., Li, D., Guo, J.P., 2016. PLAM - a meteorological pollution index for air quality and its applications in fog-haze forecasts in North China. *Atmos. Chem. Phys.* 16, 1353–1364.
- Ziková, N., Wang, Y., Yang, F., Li, X., Tian, M., Hopke, P.K., 2016. On the source contribution to Beijing PM_{2.5} concentrations. *Atmos. Environ.* 134, 84–95.
- Zhang, L.W., Chen, X., Xue, X.D., Sun, M., Han, B., Li, C.P., Ma, J., Yu, H., Sun, Z.R., Zhao, L.J., Zhao, B.X., Liu, Y.M., Chen, J., Wang, P.P., Bai, Z.P., Tang, N.J., 2014a. Long-term exposure to high particulate matter pollution and cardiovascular mortality: a 12-year cohort study in four cities in northern China. *Environ. Int.* 62, 41–47.
- Zhang, Q., Yuan, B., Shao, M., Wang, X., Lu, S., Lu, K., Wang, M., Chen, L., Chang, C.C., Liu, S.C., 2014b. Variations of ground-level O₃ and its precursors in Beijing in summertime between 2005 and 2011. *Atmos. Chem. Phys.* 14, 6089–6101.
- Zhang, R., Wang, G., Guo, S., Zamora, M.L., Ying, Q., Lin, Y., Wang, W., Hu, M., Wang, Y., 2015. Formation of urban fine particulate matter. *Chem. Rev.* 115, 3803–3855.
- Zhang, Y.L., Cao, F., 2015. Fine particulate matter (PM_{2.5}) in China at a city level. *Sci. Rep.* 5, 14884.
- Zhao, C., Wang, Y., Zeng, T., 2009. East China plains: a “basin” of ozone pollution. *Environ. Sci. Technol.* 43, 1911–1915.
- Zhao, S., Yu, Y., Yin, D., He, J., Liu, N., Qu, J., Xiao, J., 2016. Annual and diurnal variations of gaseous and particulate pollutants in 31 provincial capital cities based on in situ air quality monitoring data from China National Environmental Monitoring Center. *Environ. Int.* 86, 92–106.
- Zheng, G.J., Duan, F.K., Su, H., Ma, Y.L., Cheng, Y., Zheng, B., Zhang, Q., Huang, T., Kimoto, T., Chang, D., Pöschl, U., Cheng, Y.F., He, K.B., 2015. Exploring the severe winter haze in Beijing: the impact of synoptic weather, regional transport and heterogeneous reactions. *Atmos. Chem. Phys.* 15, 2969–2983.
- Zhou, M., Liu, Y., Wang, L., Kuang, X., Xu, X., Kan, H., 2014. Particulate air pollution and mortality in a cohort of Chinese men. *Environ. Pollut.* 186, 1–6.
- Zhou, X., Cao, Z., Ma, Y., Wang, L., Wu, R., Wang, W., 2016. Concentrations, correlations and chemical species of PM_{2.5}/PM₁₀ based on published data in China: potential implications for the revised particulate standard. *Chemosphere* 144, 518–526.
- Zou, Y., Deng, X.J., Zhu, D., Gong, D.C., Wang, H., Li, F., Tan, H.B., Deng, T., Mai, B.R., Liu, X.T., Wang, B.G., 2015. Characteristics of 1 year of observational data of VOCs, NO_x and O₃ at a suburban site in Guangzhou, China. *Atmos. Chem. Phys.* 15, 6625–6636.